THESIS FOR THE DEGREE OF DOCTOR OF PHILOSOPHY

Optimising microwave hyperthermia antenna systems

by

PEGAH TAKOOK

CHALMERS

Department of Electrical Engineering
CHALMERS UNIVERSITY OF TECHNOLOGY
Göteborg, Sweden 2018

To my lovely Faranak

*Without health life is not life; it is only a state of languor and suffering
-an image of death.*
-Buddha-

Abstract

This thesis presents the design and optimisation of a microwave hyperthermia antenna system for treatment of head and neck cancer as well as brain cancer. Hyperthermia (HT) has shown the ability to enhance the performance of radiotherapy and chemotherapy in many clinical trials. The incidence of increased tissue toxicity as a result of high radiotherapy dose has made hyperthermia a safe adjuvant treatment to radiotherapy.

Although many clinical studies have shown the effectiveness of hyperthermia for treatment of head and neck (H&N) cancer, the presence of large vessels, tissue transitions and critical tissues in the head and neck poses therapeutic challenges for treatment of advanced tumours in this region. Late side-effects of conventional therapies in treatment of brain tumours in children have made hyperthermia an attractive method. However, heating tumours in the brain is even more challenging due to the brain's high levels of sensitivity, thermal conductivity and perfusion.

This thesis presents microwave hyperthermia applicators as an efficient means to heat H&N and brain tumours. An ultra-wideband antenna, as the radiating element in microwave hyperthermia applicators, has therefore been designed, built and evaluated. The time-reversal focusing technique is used to target electromagnetic energy into the tumour. The effect of frequency and virtual source positions in the time-reversal method are studied, for different tumour sizes and positions, so as to obtain more accurate treatment planning. The optimal detailed design of the applicator, such as the number of antennae and their positions, are also investigated.

The second part of this thesis focuses on applicators for the treatment of brain tumours in children. Helmet applicators are presented and there is an investigation into how the number of antennae and their frequencies affects applicator's performance when heating large, deep-seated brain tumours. Finally, the optimum position of antennae in helmet applicators is discovered by running optimisations on simplified and realistic models of a child's head.

Keywords: microwave hyperthermia, time reversal, wideband antenna, treatment planning, head and neck tumours.

List of Publications

This thesis is based on the following papers:

Paper I.

    P. Takook, H. Dobšíček Trefná, J. Gellermann, M. Persson, "Compact self-grounded Bow-Tie antenna for UWB hyperthermia applicator", in *International journal of Hyperthermia and thermal therapies*, Vol 33, Number 4, pp. 387-400, 2017.

Paper II.

    P. Takook, H. Dobšíček Trefná, Xuezhi Zeng, A. Fhager, M. Persson, "A Computational Study Using Time Reversal Focusing for Hyperthermia Treatment Planning", in *Progress In Electromagnetics Research B*, Vol. 73, pp. 117-130, 2017.

Paper III.

    P. Takook, H. Dobšíček Trefná, M. Persson, "Experimental evaluation of UWB applicator prototype for head and neck hyperthermia", *11th European Conference on Antennas and Propagation (EuCAP)*, Paris, France, March 2017.

Paper IV.

    P. Takook, H. Dobšíček Trefná, M. Persson, "Performance evaluation of hyperthermia applicators to heat deep seated brain tumors", in *IEEE Journal of Electromagnetics, RF and Microwaves in Medicine and Biology (J-ERM)*.

Paper V.

    P. Takook, M. Persson, Massimiliano Zanoli, H. Dobšíček Trefná, "Optimization of antenna positioning for hyperthermia treatment of brain tumor", to be submitted.

Other publications not included in the thesis:

1. H. Dobšíček Trefná, **P. Takook**, J. Gellermann, J. Yang, S. Abtahi and M. Persson, "Numerical Evaluation of Clinical Applicator for Microwave Hyperthermia Treatment of Head & Neck Tumors", *Proceedings of 7th European Conference on Antennas and Propagation*, Eucap 2013, Göteborg, Sweden, April 2013.

2. **P. Takook**, H. Dobšíček Trefná, M. Persson, "A compact wideband antenna for deep hyperthermia applicator", *28th Annual Meeting, European Society for Hyperthermia Oncology (ESHO)*, Munich, Germany, June 2013.

3. **P. Takook**, H. Dobšíček Trefná, M. Persson, "A compact wideband antenna for microwave hyperthermia system", *Proceedings of Medicinteknikdagarna*, Stockholm, October 2013.

4. M. Persson, A. Fhager, H. Dobšíček Trefná, **P. Takook**, Y. Yu, T. McKelvey, J. Karlsson, X. Zeng, H. Zirath, M. Elam, "Microwave based diagnostics and treatment in practice", *2013 IEEE MTT-S International Microwave Workshop Series on RF and Wireless Technologies for Biomedical and Health-care Applications (IMWS-BIO)*, Singapore, December 2013.

5. H. Dobšíček Trefná, J. Jonsson, B. Vessman, J. Wanemark, E Woxlin, A. Hjalmarson, L. Adelback, J. Gellermann , **P. Takook**, B. Lannering, K. Blomgren and M. Persson, "Antenna applicator for microwave hyperthermia treatment of pediatric brain cancer", *Proceedings of 8th European Conference on Antennas and Propagation*, Eucap 2014, Hague, Netherlands, April 2014.

6. **P. Takook**, H. Dobšíček Trefná, A. Fhager, M. Persson, "3-D time-reversal method in microwave hyperthermia", *29th Annual Meeting, European Society for Hyperthermia Oncology (ESHO)*, Torino, Italy, June 2014.

7. **P. Takook**, H. Dobšíček Trefná, A. Fhager, M. Persson, "Evaluation of the 3D time-reversal method for hyperthermia treatment planning in head-and neck-tumors", *Proceedings of 9th European Conference on Antennas and Propagation*, Eucap 2015, Lisbon, Portugal, April 2015.

8. **P. Takook**, H. Dobšíček Trefná, A. Fhager, M. Persson, "Evaluation of 3D time-reversal focusing method in microwave hyperthermia treatment: head and neck tumors" *16th Nordic-Baltic Conference on Biomedical Engineering and Medical Physics & 10th Medicinteknikdagarna*, Göteborg, October 2014.

9. **P. Takook**, H. Dobšíček Trefná, M. Persson, "Improvements in hyperthermia applicator design for heating head tumors", *30th Annual Meeting, European Society for Hyperthermia Oncology (ESHO)*, Zurich, Switzerland, June 2015.

10. **P. Takook**, H. Dobšíček Trefná, A. Fhager, M. Persson, "Performance evaluation of dipole versus modified Bow-Tie in annular phased array applicators", *Progress In Electromagnetics Research Symposium, The 36th PIERS*, Prague, Czech Republic, July 2015.

11. A. Fhager, H. D. Trefná, **P. Takook**, Y. Yu, T. McKelvey, J. Karlsson, X. Zeng, M. Elam and M. Persson, "Microwave Technology in Medical Diagnostics and Treatment", *2015 IEEE MTT-S International Microwave Workshop Series on RF and Wireless Technologies for Biomedical and Healthcare Applications (IMWS-Bio 2015)*, Taipei, September 2015.

12. **P. Takook**, H. Dobšíček Trefná, M. Persson, "Designation of optimal frequency for multi-frequency phased array", *12th International Congress of Hyperthermic Oncology (ICHO)*, New Orleans, Louisiana, April 2016.

13. **P. Takook**, H. Dobšíček Trefná, M. Persson, "Performance evaluation of two hyperthermia applicators for deep-seated brain tumors", *IEEE MTT-S International Microwave Bio Conference (ImBioC)*, Göteborg, Sweden, May 2017.

14. **P. Takook**, H. Dobšíček Trefná, M. Persson, "Performance evaluation of helmet-like hyperthermia applicators for brain tumors", *31st annual meeting of the European Society for Hyperthermic Oncology (ESHO)*, Athens, Greece, June 2017.

15. **P. Takook**, Erika EK, Ellen Eskilsson, H. Dobšíček Trefná, M. Persson, "Prediction of tumor heatability in microwave hyperthermia applicators", *Proceedings of 12th European Conference on Antennas and Propagation (EuCAP)*, London, UK, April 2018.

Acknowledgments

Contents

Introduction

Cancer is the uncontrolled growth of abnormal cells in the body. There are more than 100 types of cancer and each is classified by the type of cell that is initially involved. In a normal process, human cells grow and divide to form new cells while the old cells die. However, when cancer develops this process breaks down. The old and damaged cells survive and new and unnecessary cells form.. These new cells can continue to grow and form masses of tissue called tumours. Malignant tumours form when cancerous cells move around the body, destroying healthy tissues. When cancer cells spread to other parts of the body, invading and destroying healthy tissues, They are said to have metastasised. This process is called metastasis and the outcome is a serious and life-threatening condition [1, 2].

Cancer is among the leading causes of death worldwide. 14 million new cases were reported in 2012 and 8.8 million cancer-related deaths worldwide in 2015 [3]. The uncontrolled growth of cancerous cells can affect any part of the body. The resulting growth invades surrounding tissues and can metastasise to remote areas of the body. Although the death rate from cancer continues to decay, cancer still remains a major health problem affecting more than 1.6 million people each year [4]. According to World Health Organization, 30-50% of all cancers could be prevented by avoiding the main risk factors such as tobacco and alcohol and by exercising regularly and maintaining a healthy lifestyle [3].

The standard cancer treatment methods include surgery, radiotherapy, and chemotherapy. These treatments may be used alone or in combination with other methods. The choice of therapy may depend upon the location and stage of the cancer and the general condition of the patient. Surgery is the longest-standing therapy for cancer and is usually combined with other modalities to improve the

treatment of tumours. This is because in many patients, simply excising a tumour is not sufficient to prevent a relapse. Radiotherapy, on the other hand, is not very effective in lower doses and can fail to treat bulky tumours. Moreover, the limited dose tolerance of some normal tissues can put the patient at risk. This means the admissible dose has to be limited and so treatment of the tumour may fail. This treatment modality may also lead to late complications and increased risk of developing secondary cancers. Chemotherapy utilises one or more anti-cancer drugs. The efficacy of chemotherapy is dependent on the type and stage of cancer. Chemotherapy may eradicate cancer if administered in the early stages of the disease when the metastasis is undetectable [5].

1.1 Hyperthermia

The disappearance of a tumour after high fever was first reported over a century ago [6]. Since the 1960s, hyperthermia has attracted considerable interest as a cancer therapy. In hyperthermia treatment tumours are heated selectively to temperatures above 40°C while healthy tissues are kept below tissue-dependent critical temperatures [7]. The rationale for using hyperthermia is that treatment at temperatures between 40 and 44°C is cytotoxic for cells in an environment with low pO2 and low pH. These conditions are found in tumour tissues with low blood perfusion. Under these conditions, radiotherapy is less effective and cytotoxic agents reach tumour areas in lower concentrations [8]. Since hyperthermia increases tumour blood flow, it increases the oxygenation of hypoxic tumours and therefore acts a radiosensitizer of the tumour [9]. Increased blood flow also leads to greater uptake of cytotoxic agents and enhances the efficacy of chemotherapy [10][11].

In a recent work by Issel et al., [12], six important features of hyperthermia have been proposed which are representing the effect of this modality to prevent tumour growth. As shown in Figure 1.1, the first effect is 'blocking cell survival'. This is based on the capability of heat to kill cells, in a correlation between time and temperature dosage. At the same time, heat can lead to thermotolerance in some surviving cells. The second effect of hyperthermia is 'inducing cellular stress response' in terms of heat-shock proteins. Heat-shock proteins are produced by cells when they are exposed to temperatures higher than normal body temperature. These proteins assist in recovery from stress by repairing damaged proteins or by impairing them. The third effect is 'modulation of immune response'. The release of heat-shock proteins carrying tumour antigens, the thermal activation of immunocompetent cells and the effects of heat on lymphocytes moving into the tumour are all involved in regulating the immune system. The fourth effect of hyperthermia is 'changing tumour microenvironment'. This covers the

physiological changes resulting from heat, the effects on tumour vasculature and the metabolic transformations. The last two effects of heat are 'evading DNA repair' and 'sensitization to radiation and chemotherapy'. The effect of hyperthermia on DNA repair has shown itself in radio-sensitization of the cells, that are deficient in repairing of DNA double-strand breaks through the homologous recombination (HRR) or non-homologous end-joining (NHEJ) repair pathways. Hyperthermia inhibits the HRR pathway after application of heat over a period of time. This provides a justification for developing anti-cancer treatments combining hyperthermia-induced HRR inhibition in tumours, with systematic application of drugs for local sensitisation of cancer cells to the DNA-damaging agents.
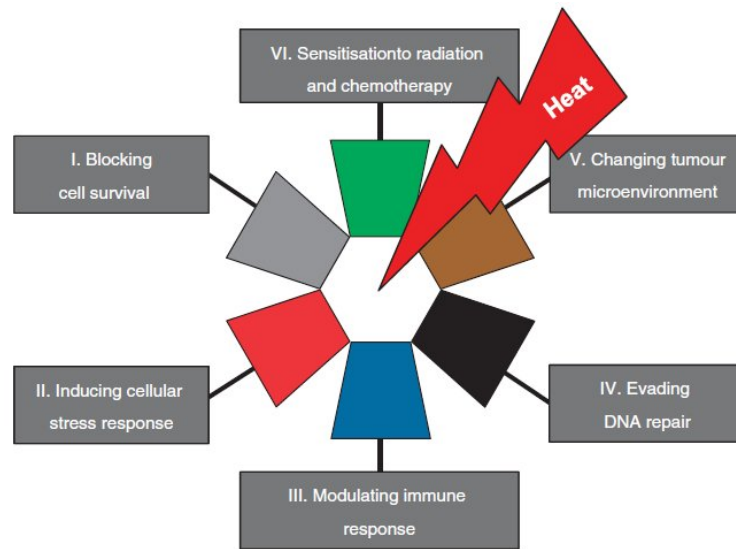
Figure 1.1: The Hallmarks of hyperthermia according to [12].

In a proposed thermal-dose relationship, it was shown that for every $1°C$ rise in temperature above $43°C$, cell killing doubles while cell killing diminishes by about one quarter for every $1°C$ below $43°C$ [13]. A method was presented that combines time and temperature to a so-called thermal isoeffective dose. This resulted in the expressions CEM_{43} and $CEM_{43}T_{90}$ which can be used to compare different tissues in terms of their thermal-dose sensitivity. A review paper by Gerard C. van Rhoon [14] discusses the relevance of CEM_{43} as a thermal-dose parameter for monitoring hyperthermia treatment. The paper mentions a number of weaknesses in the CEM_{43} concept, when used to predict the effectiveness of radiotherapy combined with hyperthermia. The effect of sensitisation by enhanced oxygenation, multiple fractions and variation in interval time have not been included in the concept of CEM_{43}. The paper proposes that further research be carried out in the field of CEM_{43}, to detect any thermal dose-effect correlation.

Clinical trials (research studies involving people) evaluate the advantages of different treatments and broaden the options available to patients. Numerous clinical trials have demonstrated the beneficial effect of hyperthermia in treating different tumour sites, when incorporated into standard radiotherapy and chemotherapy protocols [15][16]. All these studies show that adding hyperthermia makes tumour cells more sensitive to chemo or radiotherapy and thus positively affects treatment outcome. Several clinical trials have compared radiotherapy alone with combined thermoradiotherapy. These have demonstrated the benefits of hyperthermia for local control and survival in recurrent breast cancer, cervical carcinoma or H&N tumours [17][18][19][20]. Moreover, many clinical study reviews have shown the capabilities of hyperthermia to enhance cell sensitivity to radiation and drugs [22][23][8][17]. In 1997, Amichetti showed the advantages of local hyperthermia combined with radiotherapy in treating advanced squamous cell carcinoma of the head and neck (H&N). Except for mild local toxicity, no severe late side effects were observed in this study [24]. The respective benefits of adding hyperthermia to standard radiotherapy for patients with locally advanced cervical carcinoma and pelvic tumours were also shown in separate studies by Franckena et al. and Van der Zee et al. [25][26]. In the first randomised phase 3 trial by Issels et al, regional hyperthermia has been shown to increase the benefits of chemotherapy in localized high-risk soft-tissue sarcoma [27].

1.1.1 Hyperthermia in head and neck cancer

5% of all patients suffering from cancer worldwide have tumours in H&N region [28]. Annually, of 550,000 cases of H&N cancer, 300,000 cases of deaths occur. The number of males with this type of cancer is 2-4 times greater than the number of females. For H&N cancer, the most important risk factors are alcohol and tobacco consumption. Incidence of this type of cancer from infection with carcinogenic types of human papilloma virus (HPV) is also increasing. H&N cancers originate in the upper airways and swallowing tracts and are further categorized by the areas of the head or neck in which they begin. These areas, shown in Figure 1.2, are: oral cavity, pharynx, larynx, paranasal sinuses and nasal cavity and salivary glands. These cancers are the sixth most prominent cancers worldwide [3].

Management of advanced H&N cancer is challenging. For locally advanced H&N cancer, the results of phase II and III studies have shown the best standard treatment to be radiation combined with chemotherapy, albeit with added toxicity. In the treatment of these tumours, standard radiochemotherapy and chemoradiotherpay generally result in a five-year survival rate of 20-65%. This depends on the stage and location of cancer [29]. Other studies show that combined radiotherapy and chemotherapy in H&N results in an 8% increase in two-year survival.

More recently, a 4.5% increase in five-year survival has been reported [31][32]. Although survival has somewhat improved and complete response and local control in combined-modality treatments are typically high, the toxicity level in this type of tumour is severe and increases with radiotherapy doses. More than 80% of patients experience severe toxicity with current treatment methods. Increasing swallowing difficulties and decreasing saliva production have been observed in high radiation doses, which can lead to problems in speaking and eating. So, the aim should be to decrease the toxicity and increase the effectiveness of H&N cancer treatments.
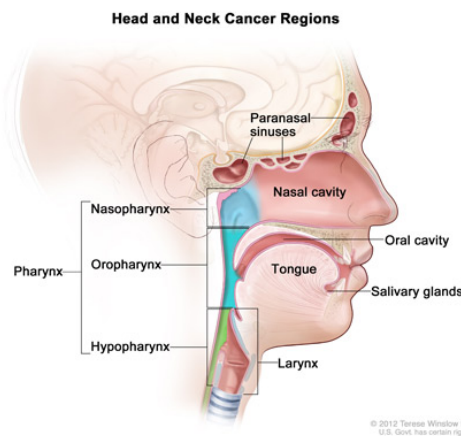
Figure 1.2: Head and neck cancer regions [1]

Enhancement in treatment outcomes of H&N cancer can be expected from combination of hyperthermia and radiotherapy. This enhancement results from an increased RT dose in the tumour and decreased RT dose in the areas at risk. In early studies by Valdagni et al., long-term follow-up of a randomised trial was used to compare radiotherapy alone versus RT plus hyperthermia, when used in metastatic lymph nodes in H&N patients. The five-year follow-up confirmed the effectiveness of combined RT and hyperthermia and also the absence of toxicity in the treatment [33][34]. Recent meta-analysis by Data et al. [16], has summarized the outcome of clinical trials in H&N cancers (HNCs) using hyperthermia and radiotherapy versus radiotherapy alone. The conclusion was that hyperthermia combined with radiotherapy enhances the probability of the complete response in H&N cancers by around 25% compared to radiotherapy alone.

Figure 1.3 shows a summary of the results of phase III randomised trials for H&N cancers. These results show a clear benefit in adding hyperthermia to standard treatment regimens [20]. In the first study, superficially located metastatic lymph nodes from the H&N received RT or RT combined with hyperthermia

(HT). The results of the treatments showed a complete response rate of 82.3% after RT+HT, versus 36.8% after RT alone. In the second study, advanced tumours mostly close to the skin were treated either by HT combined with RT, or RT alone. The results of RT+HT treatment showed significantly improved tumour control in patients with advanced tumours. In the third study, tumours in the oropharynx, hypopharynx and oral cavity were given RT or RT+HT. The complete response rate in the group with RT alone was 42.4%, whilst the HT group was on 78.6%. In the fourth study, patients with nasopharyngeal cancer were treated with chemo-radiotherapy, with or without HT. The study results showed a significant improvement in the control response: i.e. 81.1% (CRT) to 95.6% (CRT + HT). In the final study, nasopharyngeal cancer was given CRT with or without HT. The 36-month survival rate for CRT was 54% compared to 73% for CRT+HT. In addition to these clinical trials, early experiences with the HYPERcollar3D applicator were recently reported, based on the treatment of five patients with H&N tumours [21]. In these experiments, radiotherapy was followed by hyperthermia sessions once a week and invasive thermometry used, when possible, to monitor the temperature.

Different heating techniques were used in these studies. In the first study, the radiative heating was conducted in the range of 280-300 MHz using the BSD 1000 system. In the second study, capacitive heating at 27.12 KHz was applied using the Siemens Ultraterm 607E diathermia machine. In the third study, HT was applied at 8 MHz using a capacitive applicator. However, investigating the performance of the applicator showed that the applicator was not able to treat deeply located tumours. In the fourth study, a wire-based conductive heating method at 915 MHz was used to heat tumours. In the final study, hyperthermia was delivered by a capacitive applicator at 13.56 MHz or 40.68 MHz. The results of all these studies indicated improvements in radiotherapy and chemotherapy by adding hyperthermia and with no toxicity caused. However the applicators concerned were only able to heat superficial tumours and not deeply located ones. Moreover, monitoring and control of the temperature in all of these trials was limited which made it difficult to evaluate the required thermal dose. All of these results necessitate the design and development of applicators with deep-heating capability. Chapter 2 contains a more detailed discussion of the requirements for designing and developing a hyperthermia applicator with deep-heating capability for the H&N.

1.1.2 Hyperthermia and childhood brain cancer

Although there has been a considerable improvement in the treatment of cancer in general, brain cancer treatments often give disappointing results. In two decades, conventional treatment methods have failed to control tumour progression [35][36]. Of the main types of brain tumour, glioblastoma is the most com-

Reference	Tumor	Combi	N	Endpoint(s)	-HT	+HT	Heating	Quality control
Valdagni et al. 1988 & 1994 [18, 19]	Neck Nodes	RT	44	CR	41 %	**83** %	Radiative (280–300 MHz)	Invasive, > 4 each HT session (periphery:core = 4:1)
				5 years LC	24 %	**69** %		
				5 years OS	0 %	**50** %		
Datta et al. 1990 [21]	OC, OP (stage I–IV)	RT	65	CR	31 %	55 %	Capacitive, (27.12 kHz)	-
Huilgol et al. 2010 [22]	OC, OP, HP (stage II–IV)	RT	54	CR	42 %	**79** %	Capacitive (8 MHz)	Invasive (infrequent)
Hua et al. 2011 [25]	NP (stage I–IV)	CRT	180	5 years LC	79 %	**91** %	Conduction (resistive wire)	Nasal cavity internal skin temperature
				5 years PFS	63 %	**73** %		
				5 years OS	70 %	78 %		
Zhao et al. 2014 [27]	NP (stage II–IV)	CRT	83	3-years OS (QoL)	54 %	**73** %	Capacitive	Nasal cavity internal skin temperature

RT Radiotherapy, *CRT* Chemo-radiotherapy, *N* total number of included patients in the study, *−HT* results without HT, *+HT* results with HT, *LC* local control, *CR* complete response, *PFS* progression free survival, *OC* oral cavity, *OP* oropharynx, *HP* hypopharynx, *NP* nasopharynx. Results in bold are significant at the 5 %-level. Toxicity was comparable in all randomized trials, although Zhao et al. found an improved quality of life (QoL)

Figure 1.3: Results of phase III randomised trials on hyperthermia for H&N cancers [20].

mon and most fatal in adults, usually relapsing very soon after surgery. The average survival for patients with malignant glioma is only 17 weeks; this can be extended to 30 weeks after surgery and chemotherapy [37].

Studies of cancer incidences in children younger than 15 years old have shown brain tumours to be the second most common cancer, representing 20-30% of all childhood cancers. Medulloblastoma is the most common type of pediatric brain tumour. Treatments for this tumour begin with surgical excision. The addition of radiotherapy and chemotherapy may increase the disease-free survival rate. However, there are side effects from radiation treatments including cognitive damage, problems in bone growth and hearing loss [38]. Every year, 300 children in Sweden develop a malignancy, one third of which are brain tumours. While modern cancer therapies cure 75% of all paediatric cancer cases, these therapies (like radiotherapy) have been reported as having long-lasting side effects. Side-effects include intellectual impairment and perturbations in growth and puberty[39, 40].

Hyperthermia is a safe treatment, with a slow heating process and minimal damage to the surrounding normal tissue. Experiences with hyperthermia in treatment of brain tumours are limited to glioblastoma multiforme in adults. Interstitial hyperthermia combined with brachytherapy has been demonstrated as safe for this type of tumour, with no additional toxic effects [41, 42]. It was subsequently demonstrated that interstitial brain HT given before and after brachytherapy and after radiotherapy significantly improved survival of high-grade glioblastoma patients, with acceptable levels of toxicity [43]. Despite the improved treatment outcome, it was difficult to achieve the homogeneous therapeutic temperatures sought. Figure 1.4 shows how interstitial electrodes are implanted in a brain tu-

mour. In a recent study, a group of patients with malignant glioma was treated with hyperthermia in combination with radiotherapy and chemotherapy. In the study, hyperthermia was applied using a radio-frequency applicator at 13.56 MHz. Another group of patients underwent conventional radiotherapy and chemotherapy. An evaluation of the patients three months post-treatment showed glioma growth suspension and decreased tumour diameter in the hyperthermia group [44].

Figure 1.4: Electrodes implanted in a brain tumour [45].

Magnetic fluid hyperthermia (MFH) has been proposed as an alternative to interstitial HT, as it may achieve higher temperatures in intracranial tumours. This method was used to allow for more precise heating and its combination with a lower radiotherapy dosage was shown to bring about a higher overall survival rate than conventional therapies [46]. The method was shown to be safe and effective in the treatment of recurrent glioblastoma. However, this technology requires a direct injection of iron oxide nanoparticles dispersed in water. This aqueous dispersion of iron-oxide is injected directly into the tumour and then excited by alternating magnetic fields (AMF), which produces local heat in the tumour. The AMF needs appropriate field amplitude and frequency to heat up the particles. Magnetic nanoparticles (MNP) use various mechanisms to convert magnetic energy into heat energy. Some of the main heat-generating mechanisms are Néel and Brownian relaxations [47]. In Néel relaxation, heat is generated by rapid changes in the direction of magnetic moments. Brownian relaxation results from the physical rotation of MNPs in their host medium. Both of these frictions lead to a phase difference between the applied magnetic field and the direction of magnetic moment. This generates thermal loss [48]. However, these MNPs may remain in the body for life, thus hindering any future MRI scans.

Another method which can non-invasively deliver localised energy in the brain is high-intensity focused ultrasound (HIFU) [49, 50]. Specific transducers are used to concentrate the acoustic energy into a small volume. Phase array applicators are one such transducer. They provide electronic control over beam geometry and direction and can be adjusted to allow optimum power deposition. To achieve

3D control of the ultrasound beam, many small elements are placed in 2D arrays. An acoustic focus is created by controlling the timing of the transmitted wave at each element, so that all the waves arrive in phase at the desired location. For hyperthermia applications, such a system delivers small volumetric sonications from an ultrasound phased-array transmitter, destroying the intracranial lesions by thermocoagulation [49]. Nevertheless, heating large volumes (typical in paediatric brain tumours) is still demanding with present technology. Moreover, regions of the brain close to the skull continue to be a limitation for HIFU, due to heating of the skull [51] [52].

Although most of the patients treated with hyperthermia are adults, encouraging clinical results on children and adolescents are seen, as discussed in [53]. Between 1993 and 2009, 101 patients (with a median age of 5 years 10 months) were treated for: extracranial germ cell tumours, 45 patients; rhabdomyosarcomas, 23 patients; soft-tissue sarcomas, 10 patients; osteosarcomas and ewing sarcomas, 7 patients; intestinal tumours, 2 patients; other, 7 patients. Of these, 64 patients were treated for a relapse of their condition and 37 for irresectable tumours with poor response or even progress under chemotherapy. The thermo-chemo treatment followed by surgery (61) or radiation (27) given to these unfavorable patient groups resulted in 31 patients with complete response and 27 with partial response. After a median follow-up of 27 months, 45 patients had no evidence of disease, 12 were living with the disease, 41 had died from the disease and three had died of complications other than from thermo-chemotherapy. In particular, the germ-cell tumour subgroup responded fairly well to the treatment, with five-year event-free survival of 62% and five-year overall survival of 72% [53].

In another study by Wessalowski et al. [54], cisplatin-based chemotherapy combined with deep regional hyperthermia was used as salvage treatment for children and adults with refractory or recurrent malignant germ-cell tumours. Hyperthermia was applied with electromagnetic applicators of different dimensions, adjusted for infants, children and adults of different pelvic or abdominal dimensions. Figure 1.5 shows the hyperthermia applicator used in this study for a child. This study, which was administered with a 20% lower cisplatin dose in chemotherapy, resulted in an objective tumour response in 86% of patients with five-year overall survival of 72%. The clinical results of this study showed that combining HT with chemotherapy could improve the tumour response in children and adults with recurrent germ-cell tumours. The positive outcomes of combined treatment modalities using hyperthermia in brain tumours raises a demand for applicators specifically designed for heating these tumours. This becomes even more crucial in the case of children with brain tumours, where, to date, no electromagnetic hyperthermia applicator has been developed.

9

Figure 1.5: Clinical set-up for hyperthermia of a child [55].

1.2   Aim of the thesis

The results of clinical studies for different tumour sites all show the significance of adding hyperthermia treatment to standard therapies. However, in the H&N cancers, the complex geometry and the presence of large cooling vessels and highly thermo-sensitive tissues, such as the spinal cord and the brain, makes heating more challenging. Consequently, appropriate heating technology and temperature measurement tools are required to deliver an adequate thermal dose to this region. The hyperthermia equipment must provide a sufficient degree of freedom and enough resolution to allow adjustment of the power absorption pattern in the tumour and its surrounding healthy tissues. Up to now however, clinical hyperthermia has been mostly used for heating of superficial tumours in the H&N due to the convenience of heating, thermometry and clinical routines. There again, brain tumours are even more challenging to heat due to the high degree of sensitivity, thermal conductivity and perfusion of the brain.

The aim of this thesis is to develop hyperthermia applicators for treatment of H&N tumours and brain tumours and optimising the performance of these applicators. There are several ways to optimise the performance of a hyperthermia applicator. The main goal is to target electromagnetic energy into the tumour area, creating a highly localized heating region. The more energy/power deposited into the tumour, the higher the temperature elevation. At the same time, the temperature of healthy tissues should be kept below critical levels. The main design parameters of a hyperthermia applicator need to be determined and optimised in order to meet all these requirements. As it is also mentioned in the work by [56],

the important design parameters are the type, the number and the positioning of antenna elements in applicators and the operational frequency of the treatment.

Many studies have shown that significant improvement in tumour power deposition can be obtained by increasing the number of the antenna elements or antenna rings [57][58]. Moreover, the frequency of operation for optimal power density deposition depends on the size and position of the tumour and size of the area being treated. For example, the frequency of 434 MHz was chosen in the work by Paulides et al. [59] for treatment of H&N tumours, while 70 MHz was the operational frequency for treatment of pelvic tumours [60][61]. Antenna characteristics, such as their near-field radiation pattern, are also influential factors in creating a localized heating zone. Finally, the optimal positioning of the antennas in relation to each other and to the patient can lead to enhanced power deposition in the tumour.

This thesis describes the design and development of hyperthermia applicators for heating H&N tumours and brain tumours. While different design approaches have been presented for the H&N applicators and the brain applicator, all the applicators have the capability for focus-size adjustments, by adapting the power density pattern. This is achieved by optimizing the antenna elements to have wideband performance over the required range of frequencies. Increasing the number of antennas and optimizing their positioning in the applicator is the other approach we follow to achieve adequate heating in tumors. Finally, the time-reversal focusing method is employed in hyperthermia treatment planning where focused heating in tumours is planned.

The thesis is organized as follows: Chapter II introduces the requirements of microwave hyperthermia systems for deep-seated tumors and reviews the simulation techniques in hyperthermia treatment planning, emphasising the time-reversal focusing technique. Brief summaries of the papers are given in Chapter III while concluding remarks and discussions of future work are presented in Chapter IV.

Hyperthermia system

Different techniques are applied in clinical hyperthermia depending on the tumour size and position. Intracavitary, interstitial and superficial heating techniques are all included in local hyperthermia, while locoregional hyperthermia is applied to deep-seated tumours, such as tumours of the pelvis, bladder and prostate. Most clinical hyperthermia systems used in deep heating employ electromagnetic (EM) fields or ultrasound (US). There are four main parts to a hyperthermia system: treatment planning, an amplifier system, an antenna applicator and a thermometer, Figure 2.1. The water bolus and the cooling system are also parts of the applicator.

An amplifier system is used to power the EM radiation, which is then delivered to the patient via an antenna applicator. An antenna is a device which converts electrical energy into radio waves or electromagnetic radiation. Treatment planning allows the distribution of power absorbed by the body to be altered by changing the amplitude and phase of antennas in an applicator. The optimal amplitudes and phases are obtained during the treatment planning process.

A heating device for superficial hyperthermia should be able to increase the tumour temperature at a rate of 1°C per minute, corresponding to a SAR of 60 W/Kg in muscle, whilst allowing full regulation of the output power [62]. An applicator for deep hyperthermia must also meet certain minimum requirements regarding its energy distribution characteristics. The ability to focus energy distribution and control focus size and location is needed so that higher energy deposition is achieved in the tumour than in healthy tissue. A ratio is therefore defined, between the energy deposition in the target and the energy deposition in the healthy tissues. This ratio must be above 1.5 for any applicator, if that applicator is to be deemed capable of deep heating [63].

The EM fields used to heat body tissues are in the frequency range of 0.5 MHz to 2.45 GHz, covering low frequencies to microwave range. Different types of applicators were developed for this frequency range including waveguides, dipole antennas and coils. In local hyperthermia where superficial tumours are treated, different applicators are used based on the operational frequency. Capacitive electrodes and inductive coils have been used at frequencies lower than 40 MHz [64]. At frequencies greater than 400 MHz, waveguide applicators, horns, spirals and current sheets are some antennas types in clinical use. Annular-phased arrays are the most common type of applicators for regional hyperthermia, when treating deep-seated tumours. The most common phased array set up for deep hyperthermia is a circular or elliptical array of antennas arranged around the body, as shown in Figure 2.2. The desired focusing into the target is achieved by constructive interference of the radiated electromagnetic fields from the antennas [64]. The remainder of this chapter presents different types of antenna elements used in hyperthermia phased arrays.

A water bolus, as part of the applicator, is usually placed between the antennas and body surface to emit microwaves or radio waves into the tumours. The water bolus on the body surface ensures the electromagnetic coupling to the body, improves the impedance match to the tissue and is used as a method of cooling skin and other superficial tissues. The interaction of the generated EM fields with body tissues, governed by complex tissue permittivity, results in EM heating of the tissues [5].

In hyperthermia treatment planning, a 3D patient model is created and used to optimise the treatment parameters. This is done by electromagnetic and temperature simulations and results in the temperature pattern which is the goal during treatment [65]. The process of hyperthermia treatment planning is explained in more detail in the following sections. Thermometry is used to measure the temperature of the target during the treatment, in order to evaluate the quality of the clinical outcome. Invasive thermometry systems consist of temperature sensors and provide temperatures from a limited volume of the target. Among the non-invasive thermometry methods, magnetic resonance thermometry has been clinically proven as a reliable real-time temperature monitoring technique. Magnetic resonance imaging also has a higher spatial resolution and anatomical coverage per unit time compared to other methods including microwave imaging, computed tomography or ultrasound [66][67].

2.1 Basic electromagnetic theory

The theory of electromagnetic fileds can be described by a set of coupled partial differential equations well known as Maxwell's equations [68]. They have the
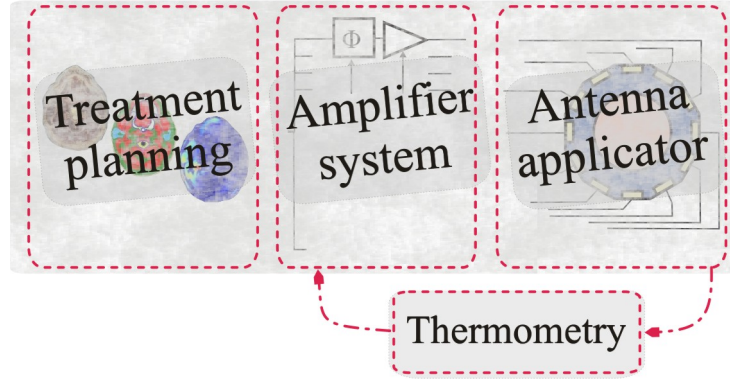
Figure 2.1: Main components of a hyperthermia system.
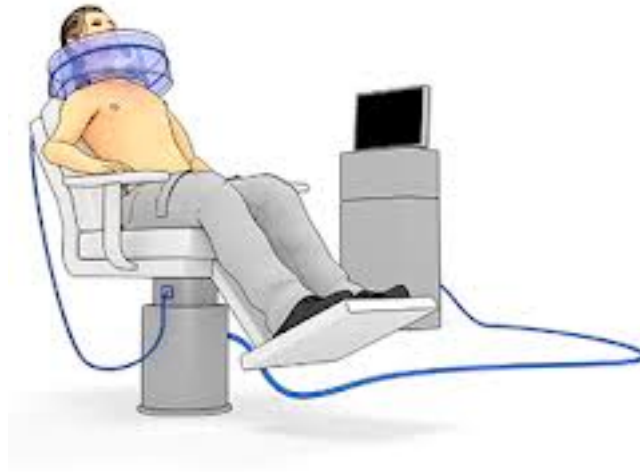
Figure 2.2: Conceptional design of H&N applicator.

following differential form:

$$\nabla \times \mathbf{E} \;=\; -\mu \frac{\partial \mathbf{H}}{\partial t} \tag{2.1}$$

$$\nabla \times \mathbf{H} \;=\; \sigma \mathbf{E} + \varepsilon \frac{\partial \mathbf{E}}{\partial t} \tag{2.2}$$

$$\nabla \cdot \varepsilon \mathbf{E} \;=\; \rho \tag{2.3}$$

$$\nabla \cdot \mu \mathbf{H} \;=\; 0 \tag{2.4}$$

where E is the electric field intensity, H is the magnetic field intensity, μ is

15

permeability, σ is conductivity, ε is permittivity and ρ is electric charge density. These four equations, together with the equation of continuity and Lorentz's force, can be used to explain and predict all macroscopic electromagnetic phenomena. By combining Eqs (2.1) and (2.2), we obtain the vector wave equation for the electric field in an inhomogeneous medium:

$$(\nabla^2 - \frac{1}{c^2}\frac{\partial^2}{\partial t^2} - \mu\sigma\frac{\partial}{\partial t})\mathbf{E}(\mathbf{r},t) = \mu\frac{\partial \mathbf{J}}{\partial t} + \frac{1}{\varepsilon}\nabla\rho \qquad (2.5)$$

where $c = \sqrt{\varepsilon\mu}$ is the speed of light. The wave equation can be further simplified by assuming a time-harmonic field as:

$$\nabla^2\mathbf{E}(\mathbf{r}) - \gamma^2\mathbf{E}(\mathbf{r}) = j\omega\mu\mathbf{J}(\mathbf{r}) + \frac{1}{\varepsilon}\nabla\rho \qquad (2.6)$$

where ω is the angular frequency in radians/second and γ is the propagation constant which determines wave propagation in different lossy media:

$$\gamma^2 = (\alpha + j\beta)^2 = j\omega\mu\varepsilon - \omega^2\mu\varepsilon \qquad (2.7)$$

Here, α is the attenuation constant and β the phase constant. As the wave propagates through a medium, the amplitude of the wave is attenuated by a factor of $e^{-\alpha z}$. The distance δ through which the amplitude of a traveling plane wave decreases by a factor of e^{-1} is called the depth of penetration:

$$\delta = \frac{1}{\alpha} = \frac{1}{\sqrt{\pi f \mu \sigma}}(m). \qquad (2.8)$$

2.2 Hyperthermia applicators

The goal of this work is to design and develop the optimum hyperthermia applicators for treatment of tumours in the H&N region and brain tumours. The applicator is one of the main components of the hyperthermia system. It therefore plays a major role in the delivery of EM energy into the tumour. The applicators must be able to effectively heat superficial as well as deeply-located tumours. In designing applicators capable of deep heating in the body, trade-offs have to be made in terms of penetration depth, focal size and size of target. According to hyperthermia quality guidelines for deep hyperthermia, the applicator should be able to reach an average SAR in the tumour. This is at least 1.5 times higher than the average SAR in healthy tissues [63].

In capacitive heating, EM fields in the range 70-140 MHz are used, with a large wavelength compared to the tumour and body size. The limited degree of control over focused power density is an important challenge for these applicators. Preferential heating of fat layers which is approximately 100 times higher than in muscle, is also a major problem. Despite these problems, reports from clinical experience have shown that an 8 MHz capacitive applicator raises tumour temperature to 42°C in superficial as well as deep-seated H&N and pelvic tumours, with minimal adverse effect [69]. Phased arrays, the most common type of deep hyperthermia applicators, were investigated in the early 1980s for HT treatment of superficial H&N tumours [70][71]. However, HYPERcollar, a phased-array of 12 antennas, was the first applicator to be developed for deep heating in the H&N region [72]. Recently, HYPERcollar3D has been developed by the same group, with more focus on integrating microwave hyperthermia into the clinic [73].

In designing deep hyperthermia applicators, the number of antennas is one of the most important factors determining the power deposition pattern in the tumour and its surrounding healthy tissues [57]. Another important factor facilitating power transfer from applicator to body is a water bolus, placed between the applicator and the patient's body surface. High power transmission values and low-power reflection values indicate good coupling efficiency between applicator and patient. Figure 2.3 shows the cross section of the Chalmers H&N applicator, including antennas, water bolus and a cross-section of the neck. The coming sections will examine the pros and cons of current hyperthermia applicators, including antenna elements and water bolus.
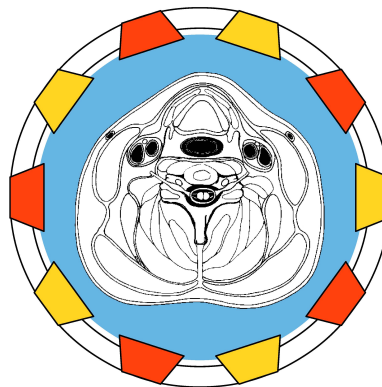

Figure 2.3: The Chalmers H&N applicator shown along a cross-section of the neck.

2.2.1 The single-antenna element

The most commonly used antennas in deep hypethermia applicators are the waveguide or dipole types. They are either filled with water or immersed in it to reduce their dimensions. Waveguides are usually filled with water, but they are large and heavy and have narrow bandwidth [74]. AMC-4 and AMC-8 are two of the existing deep hyperthermia systems, composed of 1 ring and 2 rings of 4 waveguides respectively, both at 70MHz. Due to the low operational frequency, these applicators provide a large penetration depth, with the resulting focus size usually larger than the size of the tumour. Recently, a multichannel phased array system has been produced by ALBA for deep hyperthermia treatment. The ALBA 4D system was inspired by the AMC 4/8 systems [75]. BSD2000 is a commercial deep hyperthermia system which uses dipole antennas as radiating elements in the frequency range of 75-120 MHz [76]. Sigma-Eye is a modified elliptical applicator consisting of 24 dipoles, arranged in three rings of eight antennas. The larger number of antennas in this applicator compared to its predecessor (the Sigma-60) has led to higher thermal dose in the tumour [77]. A more recent version of Sigma-Eye is compatible with magnetic resonance imaging and allows MR scans of the patient and noninvasive monitoring of deep tissue temperature [78]. However, the drawback of dipoles is the high level of power absorption resulting from their matching networks. Moreover, the omnidirectional pattern of dipole antennas makes them more prone to cross-coupling effects [79].

Patch antennas have attracted a lot of attention for use in hyperthermia, due to their low weight and because there is no need for matching networks, Figure 2.4. A probe-fed patch antenna has been designed for HYPERcollar and HYPERcollar3D phased-array applicators, which operates at 433MHz [80]. The antenna with a bandwidth of 20 MHz and a reflection coefficient $\leq$ -15 dB delivered efficient power coupling into the water bolus by using water as a substrate material. In a study by our group, a patch antenna of about 170 MHz bandwidth was designed for a wideband hyperthermia system, Figure 2.4(d). Triangular in shape, this patch antenna was excited using a probe feed and immersed in a water bolus to decrease its operating frequency. Analysis of the single antenna showed a wideband performance beyond its bandwidth, but only by using water boli of different permittivities; something that was not optimal for clinical practice [81]. The desired bandwidth of 750 MHz was achieved later by the stacked ϕ-slot design with two shorting pins, but the radiation pattern split above 750 MHz, which was not desirable [82].

In a recent study by Winter et al, a hybrid radiofrequency applicator supporting magnetic resonance imaging and MR-controlled targeted RF heating was designed and evaluated at ultra-high magnetic fields [83]. The antennas used in this hybrid applicator were dipole Bow-Tie antennas immersed in distilled water to

shrink their effective length. The building block of the Bow-Tie antenna had a dimension of $156 \times 70 \times 68$ mm3 resulting in a 3dB bandwidth of 143 MHz at the excitation frequency of 298 MHz. In this thesis, modified Bow-Tie antennas are presented as the antenna elements used in the hyperthermia applicators. The characteristics of this single Bow-Tie (SGBT) antenna are compared with those of dipole, patch, waveguide and the recently-used Bow-Tie antennas and are given in Table 2.1.

(a)   (b)

(c)   (d)
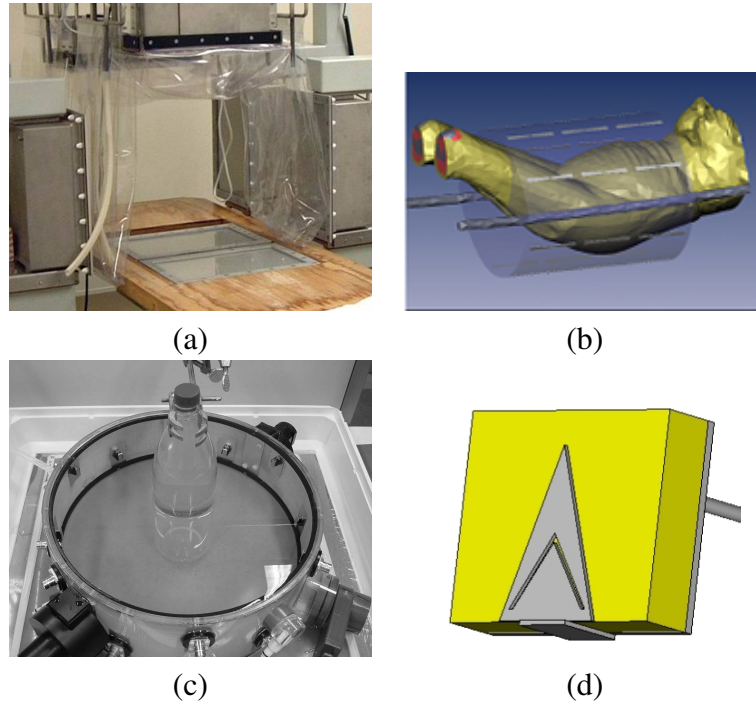
Figure 2.4: Antenna elements for hyperthermia applicators, (a) Waveguide antenna (b) Dipole antenna (c) Patch antennas in a two-ring measurement set-up [80] (d) Triangular patch antenna [81].

2.2.2 Water bolus

Water bolus is an important part of hyperthermia applicators and has a profound effect on the heating pattern of the antennas. In most cases, the space between the applicator and the patient is filled with water to improve coupling into the patient and reduce stray fields. Furthermore, the surface temperature can be controlled by circulating the water at low temperature. The water is typically encased in plastic bags in a closed water bolus system. The efficiency of the power coupling between applicator and patient can be changed by varying the thickness and shape

Table 2.1: Typical characteristics of different antennas in a hyperthermia applicator. In the table RP = radiation pattern, BW = bandwidth, Di = directional, OmDi = omni-directional, SemDi = semi-directional, MC = matching circuit, AP = aperture size, Pol = polarization, Dim = dimension.

	Waveguide	Dipole	Patch	Bow-Tie in [83]	SGBT	Desired antenna
S_{11}	$<$-25 dB	$<$-10 dB	$<$-10 dB	$<$-10 dB	$\approx$-10 dB	$\leq$-10 dB
RP	Di	OmDi	SemDi	Di	Di	Di
BW (MHz)	Few	More than a few	$\approx$ 20	143	$\approx$ 570	600
MC	No	Yes	No	Yes	Yes	No
Pol	Linear	Linear	Linear	Linear	Linear	Linear
Dim (mm)	AP 80×340	Length 30.75	27.8×10	156×70	24×27	

of the water bolus. In early modeling works of H&N applicator design, a cylindrical set up of antennas was considered in an infinite water bolus. The infinite bolus was later modified to a closed water bolus in the HYPERcollar applicator [72], with the bolus inflated with distilled water which was allowed to circulate. Another alternative, the open water bolus system, has been used in Coaxial TEM applicators [85]. These applicators are designed for treatment of deep-seated tumours in the pelvic region, with the patient surrounded by water from their toes to their upper chest. This approach provides optimal skin cooling, but without pressure on the patient from the weight of the water bolus. The major disadvantage of this concept is the limited access to the patient during the treatment, plus the significant losses.

In today's hyperthermia systems, water bolus is an integral part of antennas applicators. This makes for easy positioning of the applicator around the target. The predictability of water bolus shape is an extremely important factor affecting treatment planning performance. In the ALBA 4D system, two water boli filled with circulating distilled water are independently and remotely thermos-regulated. They are placed between patient and antennas, for signal coupling and superficial cooling [75]. In the new deep hyperthermia system by Pyrexar medical, BSD 2000 3D/MR, water bolus is an integral part of the applicator, with circulated water providing temperature control for patient comfort [76]. In HYPERcollar3D, predictability of the bolus shape was improved by splitting the water bolus into

an inner flexible section attached to the body and a stiff outer section, where the antennas are immersed [73]. This type of bolus can conform to skin contours.

2.3 Hyperthermia treatment planning

Hyperthermia treatment planning is defined as the process that begins with obtaining patient models and creating a set of quality indicators to maximize the treatment quality using electromagnetic or thermal modelling [65][86]. Figure 2.5 illustrates the HTP process which begins with determining the geometry and tissue properties of the relevant body part. The computed tomography (CT) or magnetic resonance (MR) images of the relevant body part are segmented to give an accurate, patient-specific model. The electrical and thermal properties are then assigned to each tissue. In the next step, the power density (PD) and SAR distribution are computed using a combined model of the applicator and patient. In addition to an accurate patient model, a precise applicator model is necessary for quality of treatment planning. The applicator modelling includes the geometry of the applicator and water bolus, plus electromagnetic modelling of the antenna excitation and accurate meshing. After determining the PD, the temperature distribution can be predicted considering physiological conditions such as perfusion. Finally, optimization methods are employed to maximize the power distribution or temperature in the tumour while minimizing it in remaining healthy tissues. This is done by defining several objective functions and determining the optimal amplitude and phase settings for each antenna in the applicator.
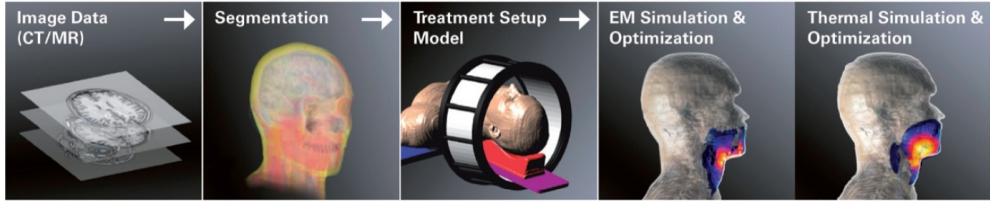
Figure 2.5: Process of hyperthermia treatment planning using electromagnetic simulation and optimization [86].

2.3.1 Numerical methods

Numerical techniques are used to solve the Maxwell equations and calculate the internal electric fields within the body in hyperthermia treatment. The most common numerical techniques in electromagnetic modelling are finite difference time domain (FDTD) and finite element method (FEM). These are used to compute the

electromagnetic fields generated by antenna applicators. FDTD is formulated on a Cartesian grid and discretises Maxwell's equations in the time domain. In FEM, the domain of interest is subdivided into small sub-domains and the field solution expressed in terms of a low-order polynomial on each of the sub-domains. FEM is efficient in terms of the cell numbers, but mesh generation in this method is time-consuming. On the other hand, FDTD is simple to perform and needs less memory when dealing with large computational domains. Mesh generation is also simple in FDTD and its parallel nature makes it suitable for acceleration techniques.

In this thesis, majority of modellings and simulations have been carried out in CST microwave studio with a transient solver as the solver of choice [87]. The ability to perform real-time domain simulations in this software enables us to study the propagation of the field through the body. The finite integration technique (FIT) is used to numerically solve electromagnetic field problems by applying Maxwell equations to a set of staggered grids. Another important feature of this solver is delivering broadband frequency domain results, such as S-parameters. These are useful in studying the reflected and absorbed power-loss values using an antenna applicator. The calculation of fields at many frequencies from just one simulation run also increases the computational efficiency. The transient solver also applies advanced numerical methods for accurate modelling of small and curved structures without extreme refinement of the mesh.

2.3.2 Patient modelling

Power density and temperature distribution are strongly dependent on 3D patient modelling. Segmentation algorithms are required to delineate tissues from CT or MR data and derive 3D patient models. The tissues are often manually segmented by clinicians in a time-consuming process. Automatic segmentation tools have been developed to speed this process up. An automatic segmentation algorithm for CT images of the head and neck was recently presented and evaluated. This algorithm improves reproducibility and reduces segmentation time [88].

Although current clinical practice in hyperthermia treatment is based on CT images, magnetic resonance imaging produces higher levels of soft-tissue contrast compared to CT. Current studies are investigating the use of MRI in addition to CT for patient modelling in H&N hyperthermia treatment planning [89].

To facilitate the use of the dielectric data in Maxwell equations, it is better to express their frequency dependence as parametric models. The characterization of the dielectric properties of biological tissues was comprehensively reviewed by Foster and Schwan [90]. In the literature review by Gabriel et al, dielectric properties of biological tissues were extracted from the literature and presented in graphical format [91]. These dielectric properties were characterized experimen-

tally in the frequency range of 10 Hz to 20 GHz [92]. A parametric model was then developed to describe the variation of dielectric properties as a function of frequency [93]. In this model, the dielectric spectrum of a tissue is characterized by three main relaxation regions and other minor dispersions. In its simplest form, each of these relaxation regions presents a polarisation mechanism characterized by a single time constant, τ. This is expressed by the so-called Debye expression, as a function of frequency. Hurt also modeled the dielectric spectrum of muscle to the summation of five Debye dispersions plus a conductivity term [94]. The broadening of the dispersion could be accounted for by addition of a distribution parameter, called α. Accounting for the dispersion expansion, the Cole-Cole equation was introduced as an alternative to the Debye equation [95][96]. Therefore, multiple Cole-Cole dispersion is more appropriate to describing the spectrum of a tissue:

$$\hat{\varepsilon} = \varepsilon_\infty + \sum \frac{\Delta\varepsilon_n}{1 + (j\omega\tau_n)^{(1-\alpha_n)}} + \frac{\sigma_i}{j\omega\varepsilon_0} \tag{2.9}$$

In equation 2.9, $\hat{\varepsilon}$ is the complex relative permittivity, σ_i is the static ironic conductivity, ε_0 is the permittivity of free space and ε_∞ is the permittivity at field frequencies where $\omega\tau \gg 1$.

Another important issue in hyperthermia treatment planning is uncertainty of the dielectric and thermal modelling parameters. If these parameters have limited precision, the uncertainty of the parameters affects the power and temperature calculations. Dealing with these uncertainties is necessary if there is to be a robust system design. In a study by Greef [97], the role of dielectric and combined dielectric and perfusion uncertainty on optimization was investigated by means of HTP for six different systems: 70 MHz AMC-4 and AMC-8, 130 MHz version of AMC-8, a three-ring AMC-12 system, the BSD SigmaEye applicator and a dipole applicator of 18 channels. The impact of dielectric uncertainty on optimization was found to depend on the number of channels/antennas in the system. The optimization results showed greater sensitivity of the optimization to dielectric uncertainty when the number of channels increased. Considering the increased complexity of a system with more channels, AMC-12 was found to be the best compromise between heating efficiency and robustness. The optimisation method of this study was temperature-based. In the following sections, power-density-based and temperature-based optimisation techniques in HTP are explained in more detail.

23

2.3.3   Power-density-based optimisation

In the most common type of deep hyperthermia applicators, the phased arrays, focusing into the target can be achieved by constructive wave interference of the electromagnetic fields radiated by antenna elements. In this process, hotspots (which are often caused by electric field maxima at boundaries with high dielectric contrast) need to be minimised. This is usually done by different optimization methods, such as the generalized eigenvalue method [98][99], genetic algorithm [100] or particle swarm optimization followed by line search [101]. While the generalized eigenvalue methods are fast, Genetic algorithms (GA) are usually slower and can not find a globally optimal configuration. However GAs are able to find settings less sensitive to antenna-steering uncertainties [86]. Particle swarm optimization is used when more flexibility in the formulation of the optimization function is needed. This optimization has shown to be effective in clinical implementation [101].

The optimization process begins after calculation of the electric fields. In the optimization of the power density (PD) or specific absorption rate (SAR), the amplitudes and phases of the sources are computed to give high PD/SAR in the target and low PD/SAR in healthy tissues. In a phased array of N antennas, the SAR distribution at a voxel r is:

$$SAR(r) = \frac{\sigma(r)}{2\rho(r)} |\sum_{i}^{N} E(r)_i V_i|^2 \qquad (2.10)$$

where SAR is the power absorbed per unit mass at the voxel r, $E(r)_i$ is the E-field for antenna i, $\sigma(r)$ and $\rho(r)$ are conductivity and density at position r, and the vector V is a complex vector showing the amplitudes and phases of each antenna.

In 1991, Sullivan presented a mathematical method for treatment planning in deep regional hyperthermia using the Sigma 60 applicator [102]. To accelerate a relatively computationally intensive optimization, he took advantage of the superposition of E-fields while dividing the whole computational domain into four quadrants. He used the impulse response method, in which one computer run was enough to calculate the E-fields at frequencies of interest. In this method, the ratio of the average SAR in the tumour to the average SAR in the body was used to quantify the output. Based on the calculated SAR ratio, the amplitudes and phases of the antennas were manually changed by the operator until the best SAR ratio was found.

Another method of optimization is the generalized eigenvalue method. This has been used as a fast optimization method to find amplitudes and phases of phased arrays in regional hyperthermia [99]. In this method, based on the basic equations for the electric field, power and temperature distribution, appropriate

objective functions are defined for optimization of power density or temperature distribution. The function for optimizing power density was defined as the quotient of the energy absorbed in the tumour region to the energy absorbed in healthy tissues. Maximizing this function leads to a solution of a generalized eigenvalue problem. Bardati carried out SAR optimisation by maximizing the SAR in the tumour and minimizing it in healthy organs [98]. The best array feed for each target (tumour/healthy tissues) was found by solving an eigenvector problem defined for that target. The optimal excitation setting resulted from a trade-off of the best array feeds.

In the work by Siauve et al. [100], a genetic-algorithm method was used to optimise amplitudes and phases of n antennas in the applicator and consequently to optimise the resulting SAR distribution. In this context, the genetic-algorithm method followed the principles of evolution through natural selection to maximize the defined objective functions. Six different SAR-based objective functions were evaluated and compared with each other in terms of the power density value inside the tumour. The genetic algorithm in this work was based on a finite element formulation.

2.3.4 Temperature-based optimisation

A temperature-based optimisation is usually based on optimisation of power deposition before calculating of the temperature distribution. The inclusion of non-linear thermal models means that extensive numerical simulations are required for the optimisation to be carried out. The common method for thermal modelling in hyperthermia treatment planning is Pennes' bio-heat equation, (PBHE)[103]:

$$c\rho \frac{\partial T}{\partial t} = \nabla.(k_{tis}\nabla T) - c_b W_b (T - T_{art}) + P \qquad (2.11)$$

where c is the specific heat capacity, ρ is the tissue density, T is the temperature, t is the time, k is the thermal conductivity, W_b is the volumetric blood perfusion and T_{art} is the local arterial temperature. The deposited power density by antennas $P(Wm^{-3})$ is calculated from the total E-field distribution. Assigning different thermal properties to different tissues is used to model the heterogeneity in tissue properties. Heat transfer between large vessels and tissue and direction of blood flow are not considered in this model, which can lead to inaccuracies in temperature evaluation. The most common numerical method for implementing the PBHE is based on the FDTD method. Since the PBHE is an approximate model, several modifications have been suggested for PBHE considering temperature-dependent non-linear effects on thermal tissue properties. One of these modifications is to use temperature-dependent parameters. In [104], a temperature-dependent blood perfusion model is used to improve the classical

bio-heat term. As with blood perfusion, the reason for choosing temperature-dependent tissue parameters is that, when heating tissues up to 41-43 °C, the blood flow in normal tissues increases significantly whilst decreasing in the tumour. In the other modified PBHE model, effective conductivity, k_{eff} is incorporated as a function of perfusion and an empirical factor [105]. In this work, comparison of different bio-heat models with the measurement results showed that, in the model with effective conductivity, conduction was found to be an important heat removal mechanism.

To model discrete vasculature, a complex thermal method (DIVA) has been developed which describes vessels as 3D curves [106]. Although this model has been validated in isolated animal organs, complexity in modelling 3D vascular networks results in long computation times. This makes the method impractical for clinical application. New methods have been developed for fast calculation of the steady-state temperature distribution and temperature-based optimization, based on the DIVA model and suitable for regular use in treatment planning [107][65]. While calculation of the steady-state temperature distribution in the original DIVA model took about 3.3 hours, it took about 1.5 hours with the fast method presented in [107]. Optimisation results with discrete vasculature modelling were also compared to the optimisation results from Penne's bioheat equation. This resulted in variation of antenna powers by a factor of 2, demonstrating the importance of taking into account the discrete vasculature model during the optimisation.

Temperature-based optimisation techniques to find the optimal phases and amplitudes of phased-array systems are more clinically suitable than power-density-based optimization. This is because temperature-based optimisation techniques take into account parameters such as thermal conduction and perfusion in the optimisation process. In a study by Greef [108] (analysing the effect of perfusion uncertainty on optimisation in HTTP), the performance of four power-based optimisation methods was compared with a constrained temperature-based optimisation, using T90 as the measure of thermal dose. Temperature-based optimisation results showed 1°C difference from the optimum solution, while deviations for the SAR method were up to 2.9°C. It was concluded that temperature-based techniques are preferable to SAR-based alternatives.

Quality indicators

The quality of a hyperthermia treatment is strongly affected by SAR in the target and by SAR peaks outside the target (known as hotspots). The SAR values in the target and the hotspots are therefore very important in analysing SAR distributions. While the SAR in the tumour needs to be maximized to raise the tumour temperature, hotspots have to be minimized to prevent patient discomfort during

the treatment.

A literature survey by Canters et al. evaluated various quality indicators in terms of their correlation to the temperature increase in the tumour [109]. $T50_{target}$, the median target temperature, was used to evaluate the SAR indicators for the purposes of characterisation and optimisation.. The reason for choosing $T50_{target}$ was its insensitivity to any temperature deviations which might have disturbed the evaluation. The indicators which were most useful for characterisation had a close correlation with the target temperature ($T50_{target}$). This means that a high value in these quality indicators equates with a high target temperature. Moreover, a suitable SAR indicator which is used as the goal function of the optimisation should lead to an optimal $T50_{target}$. Based on these evaluations, two indicators were found to be most appropriate. The first, $SAR_{hs-targratio}$, is defined as the ratio of the SAR exceeded in 1% of a region's volume and the median target SAR. This objective function, which is used to compare the highest SAR values in healthy tissues to the tumour SAR, is the most useful for hotspot reduction and optimisation procedure. The second indicator, SAR_{targ}, is defined as the averaged SAR in the tumour and is most useful in comparing absolute SAR values.

To evaluate the quality of SAR distributions, the hotspot quotient ratio (HTQ), similar to $SAR_{hs-targratio}$, was defined in Canters [110]:

$$\text{HTQ} = \frac{\text{SAR}(V_1)}{\text{SAR}_{\text{tumour}}} \qquad (2.12)$$

Here $\text{SAR}(V_1)$ is the average SAR in the first percentile of the highest SAR values in healthy tissues and $\text{SAR}_{\text{tumour}}$ is the average SAR in the tumour. In this study, the effect of patient position variations and inaccuracies were evaluated in context of SAR distribution robustness. For ten patient models tested in this work, HTQ values varied between one and five. HTQ has also been used as the goal function for optimizing SAR distribution in hyperthermia treatment planning [111]. In [111], the potential of SAR steering in VEDO software was demonstrated by analysing the first treatment using the HyperCollar. In the software, the relative amplitudes and phases of each antenna were optimised to minimize the goal function, HTQ. As the goal function, HTQ has been employed to maximize the SAR in the tumour and minimize the SAR in healthy tissues.

It is known that time and temperature have a direct effect on the rate of cell killing during hyperthermia treatment. To date, various methods have been suggested for expressing the time-temperature data in a common unit, allowing comparison of different heating regimes. This is particularly important for clinical hyperthermia, where temperature distribution is not uniform spatially and not stable temporally [112]. In [112], basic concepts relating temperature and time to cell killing and tissue damage are presented.

27

Thermal dosimetry measures that are most often reported in the literature include: T_{90}, T_{10} and T_{50} as temperature parameters; cumulative time above 40°C, 41°C, 42°C and 43°C as time parameters; cumulative number of equivalent minutes at 43°C (CEM43); cumulative equivalent minutes at 43°C at the T_{90} temperature as thermal dose parameters [113]. Here, T_{90} is defined as the tissue temperature exceeded by 90% of all temperature measurements, T_{50} is the temperature exceeded by 50% of the measured points in the tumour and T_{10} is the temperature exceeded by 10% of the measured points in the tumour. In clinical application of the thermal isoeffect dose (TID) concept, different heating protocols for different times at different temperatures are converted into equivalent minutes at 43°C. For several heat treatments in the clinic, the TIDs for each can be added to give a cumulative number of equivalent minutes at 43°C, CEM43. For example, the threshold for thermal damage in a sensitive brain in terms of EM43°C is about 30-50 minutes while, for more heat-tolerant muscle tissue, this threshold is 240 minutes.

2.3.5 The time-reversal method

Time reversal method is based on the time-symmetric property of the wave equation in a nondissipative medium. It was first introduced by Fink et. al for ultrasound [114] and later for electromagnetics by Trefna et. al [115]. The time-reversed process starts with the radiation of a pulse from a point-like source at position r_0. A cavity surrounds the source at which the time dependence of field components are measured. In electromagnetics, time-reversed wave fields inside the volume of the cavity are obtained by time-reversing the E-fields and radiating them from the cavity surface. This corresponds to the transformation of $E(r,t) \to E(r,T_0-t)$. These time-reversed fields are back-propagating by means of monopolar or dipolar sources covering the surface [116]. Considering the source function as a Dirac distribution, the time-reversed electric field is given as:

$$E_{TR}(r,t) \propto G(r_0,r,-t) - G(r_0,r,+t) \tag{2.13}$$

where $G(r_0,r,t)$ is the causal and $G(r_0,r,-t)$ is the anticausal Green's function. The interference of the converging and diverging waves results in a focal spot with a maximum size of $\lambda/2$. The focus size limit results from the Fourier transform distribution of the E-field, which is proportional to the imaginary part of the Green's function:

$$G(r_0,r,\omega) = \frac{e^{-jk\|r-r_0\|}}{4\pi\|r-r_0\|} \tag{2.14}$$

28

and

$$\mathrm{Im}G(r_0, r, \omega) \propto \frac{sin(k\|r - r_0\|)}{\|r - r_0\|}, \qquad (2.15)$$

where k is the wave number.

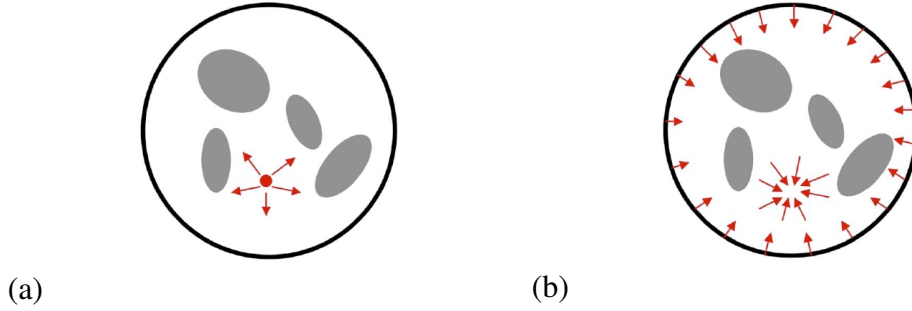(a)   (b)

Figure 2.6: The principle of the time-reversal method. (a) The recording step (b) The time-reversed step.

The time reversal theory can be used to focus the power absorption in the tumour volume. The advantage of time reversal in hyperthermia treatment planning is the speed of the method and its suitability for pulsed and continuous excitation. As explained in the HTP section, for general optimization methods, calculating the EM fields of all the antennas in the patient model is necessary to find the optimal amplitudes and phases for the antennas in HTP process requires. This process is very time-consuming due to the computation time for a single iteration. Unlike the traditional optimization methods, there is no need to calculate the E-fields of all the antenna elements in the applicator. To minimize power absorption in healthy tissues, it is necessary to incorporate hotspot reduction techniques in the treatment planning process.

In the first step, the modelling part, one or more sources are placed in the tumour volume. The optimum position of the virtual source is where the maximum tumour coverage can be achieved. The optimum position depends on the size and position of the tumour plus the frequency of treatment, as shown in Paper II. The simulated E-fields are recorded by electromagnetic models of the antenna elements. In the second step, the treatment, the antenna elements transmit the recorded field in time-reversed order. The time-reversed signals are then focused on the position of initial sources in the tumour due to the time-symmetric property of the wave equation in a lossless medium.

The time reversal focusing method has been evaluated for hyperthermia treatment planning of 2D models of the neck and breast by our group [115]. The method was implemented by 2D FDTD algorithm and the 2D models immersed in a background of water. The performance of the focusing method was evalu-

ated by quantifying the power absorption distribution in tumour areas, in terms of several parameters. The parameters studied were: the type of antenna excitation, the number of antennas in the applicator and the frequency. Although the 2D time reversal method worked well for 3D predictions [81][115], there were limitations when modelling more than one ring applicator in 2D modelling. This limitation can be obviated by a 3D implementation of the time reversal method using the FDTD algorithm as presented in Paper II.

The applicator design

This chapter discusses our approach in designing a compact UWB antenna element for hyperthermia applicators and the design process of hyperthermia applicators. An important objective is that the designed applicator should be able to heat deep as well as superficial tumours. One way of achieving this is to build in the capability to switch between multiple frequencies in the desired frequency range. This ability enables us to reach centimeter-scale spatial resolution by using higher frequencies and reach high penetration depths at lower frequencies. Another important design criterion is to use a large number of antennas. This requires the antennas to be small. The latter is also beneficial in controlling the focusing capability of the system that is designed. As discussed in section 2.1, the antenna elements in our applicator should be designed to have wide-band performance with low reflection coefficients, high penetration ability and high effective field size over the whole band. Moreover, the antenna elements should be compatible with the magnetic resonance device, which is required for non-invasive thermometry [117].

3.1 Conceptual design of the antenna element and water bolus

The antenna design discussed in this thesis is mainly based on the Bow-Tie antenna, with wide-band performance and stable radiation characteristics across the frequency range of 430-1000 MHz. The reason for designing the antenna in this frequency range is that it has been shown to be efficient in treatment of H&N tu-

mours [81][115]. Moreover, the self-grounded Bow-Tie design was selected due to its directional radiation pattern over a wide frequency band, plus its small size. To reduce the size of the single antenna, it is immersed in water. The specifically designed shape of the water bolus plays a significant role in improving the heating efficiency. In addition to the limited-size water bolus of the antennas, an extra water layer between the antennas and the patient is used for direction of electromagnetic energy into the body and for cooling the patient's body surface during treatment. More details on design and analysis of the antenna are presented in Paper I.

The sensitivity analysis of the antenna performance versus the size of the water bolus was further investigated by scaling the conical AWB, but keeping the size of the antenna and the dielectric layers fixed. The performance of the antenna was evaluated in the same setup as presented in Figure 4.1(b), by finding the S_{11} parameters versus the frequency. The calculated reflection coefficients, or S_{11} parameters for different AWB sizes are shown in Figure 3.1. Here, we scaled the AWB while keeping its height constant at 25 mm. The smallest and largest simulated AWBs are shown in Figure 3.2. The results presented in Figure 3.1 are summarized in Table 3.1, in terms of the resulting bandwidths when $S_{11} \leq$ -10dB. As shown in the table, the lowest obtained operational frequency is about 440 MHz for a scale factor of 1.2, while the maximum obtained frequency is about 920 MHz for a scale factor of 0.84 . This showed that the sensitivity of the S_{11} variation relative to the variations in AWB size is not significant. The other important conclusion was derived by finding a relationship between the length of the dipole and the operational frequencies of the antenna for different AWB sizes. As shown in Figure 3.1, the lower operational frequencies for K = 1, 1.2, 1.4, 1.8, 2.4 and 3.4 vary between 440-480 MHz. The wavelengths at this frequency range, considering water as the dielectric medium, vary between 70-77 mm. Moreover, the total length of the dipole radiating arms is about 40 mm. This shows the dipole length to be approximately equal to half the wavelengths at the lower operational frequencies of the antennas for different K values.

3.2 Head and neck applicators

Due to differences in anatomy and dimensions of the head and neck, two exchangeable applicators were developed; one for treatment of head tumours and one for the tumours in the neck. Treating neck tumours (such as laryngeal tumours) with a large applicator could result in the appearance of hotspots in other tissues, such as the chin or shoulders. The presence of hotspots in these regions is due to the transition between bone, which has low conductivity, and other tissues with higher conductivity values. Since the neck is smaller, fewer antennas ele-
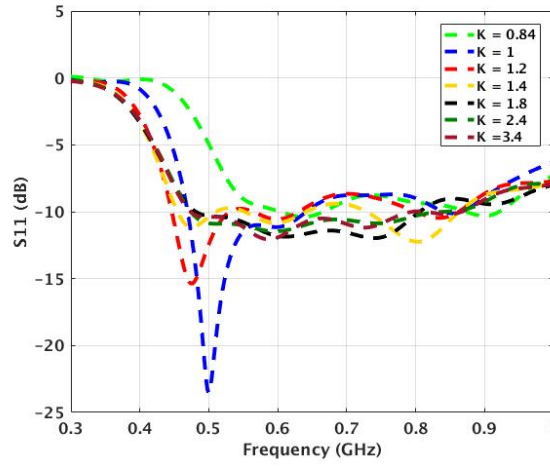
Figure 3.1: S11 variation versus different cone size, the height of the cone is fixed at 25 mm.
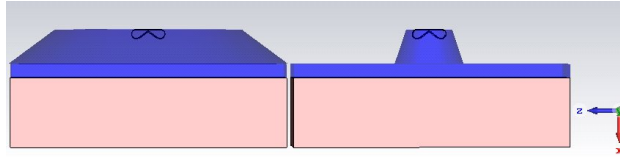

Figure 3.2: From left to right, the largest and smallest simulated AWB.

Table 3.1: -10dB bandwidth of the Bow-Tie antenna immersed in conical water boli of different size. K shows the scaling factor for the top and bottom cone diameters.

	BW (MHz)
K = 1	[460 - 870]
K = 1.2	[440 - 870]
K = 1.4	[450 - 860]
K = 1.8	[480 - 800]
K = 2.4	[470 - 820]
K = 2.8	[470 - 860]

ments will suffice. The applicator consists of 10 antennas of adjustable diameter. In designing the head applicator, we must take into account the larger size of the head and the presence of complex anatomical structures.

By investigating the effect of the number of antennas and the radius of the

33

array relative to the neck size on a cylindrical muscle phantom, it was found that 10 antennas in a circular array of 100 mm-radius provided the best focus in the phantom. Thus, the optimal neck applicator consists of 10 antennas arranged in one ring. The same investigation was carried out to find the optimal number of antennas and size of the head applicator in cylindrical and elliptical muscle phantoms. This resulted in an elliptical applicator consisting of 16 antennas arranged in two rings and with radii of 104 mm along the X axis and 114 mm along the Y axis. In both applicators, water boli of thickness 1-2 cm are placed between the body and the applicator.
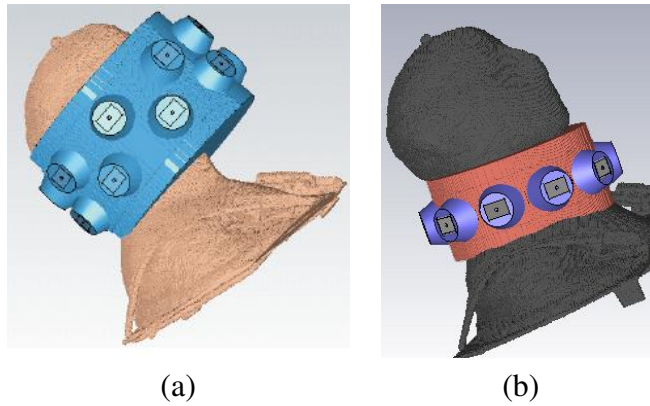

(a) (b)

Figure 3.3: The applicators for (a) head and (b) neck tumours shown on anthropomorphic phantoms of head and neck.

3.3 Brain applicator

As discussed in section 1.2, hyperthermia in addition to standard modalities has been shown to enhance the treatment outcome of brain tumours. To apply hyperthermia, applicators capable of heating the brain tumours are required. The principle of annular phased arrays can be applied to the design of intracranial applicators. However, applicators of a helmet-shaped design are more beneficial due to their higher degree of tumour coverage. This is because extra radiation reaches the tumour from a third dimension.

An initial design of the head applicator was presented in [118] for treatment of intracranial tumours in children. The helmet-shaped applicator consisted of 15 antennas in two rings of eight and six elements, with one antenna located on top of the head. As shown in figure 3.4, all the antennas were tilted according to the head shape. The surface water bolus consists of three strips of 7 cm wide and 2 cm thickness. Although the SAR distributions obtained for different tumours

were favorable, the T_{50} of $38°$ was somewhat disappointing for treatment of large tumours such as medulloblastomas [118]. There are two alternative solutions in tackling this challenge. The first is to decrease the operational frequency band of the antennas and improve the penetration depth of EM waves. The second is to substantially increase the number of antennas used and is the approach followed in Paper III. This paper compares the performance of three helmet-shaped applicators, for heating large, deep-seated brain tumours in children.
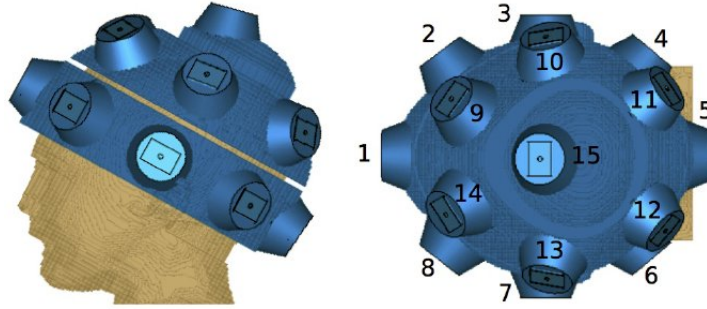

Figure 3.4: Initial design of a child head applicator consisting of 15 antennas.

As shown in Paper III, the power deposition in the tumour is proportional to the number of antennas in the applicator. An initial design was therefore considered, of a helmet-shaped applicator with 50 Bow-Tie antennas. These antennas were placed over a 10 mm water layer, surrounding a spherical phantom of radius 100 mm, approximating the size and shape of a child's head (see Figure 3.5(a)). The phantom had tissue properties of brain grey matter and the dielectric properties of the biological tissues were extracted from the IT'IS database [119]. The antennas employed in the applicator were regular Bow-Tie antennas immersed in reduced-size conical water boli with a wide-band performance over 500 MHz-1 GHz.

The heating capability of hyperthermia phased arrays have been investigated, in terms of power to the tumour and other figures of merit, in the work by Bardati et. al. [120]. This work assumed that each antenna is limited to a maximal nominal power. Under such constraints, they proposed new methods to maximize the power-to-tumour ratio and heating efficiency. To characterise the heating performance of the applicators, we took a different approach by using a new algorithm to search through the whole phantom model (head/brain) and find the easiest/most difficult place to heat. This information allows us to know if a specific applicator design is able to heat a tumour at a specific position in the head. The search results in this algorithm are based on the value of hyperthermia quality indicators aPA, RTMi and HTQ. In the current design, HTQ is considered as the basis of our search results. As shown in Figure 3.5 (b), the algorithm goes through all the voxels in the head, considering each voxel as a focus point. Using the calculated

E-fields of the antennas in the applicator at a specific frequency, the power-loss density and specific absorption rate (SAR) are computed. Finally, by computing the quality indicators at each voxel, the easiest/most difficult places to heat in the phantom were found.
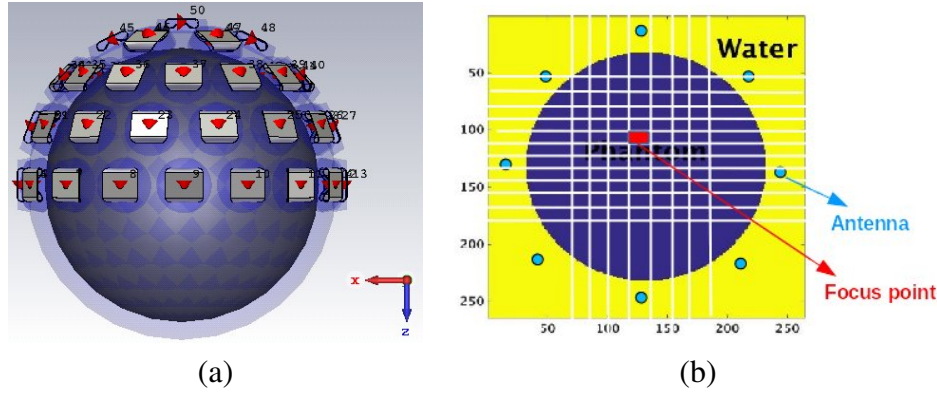

Figure 3.5: (a) Helmet-shape applicator with 50 antennas (b) Cross-section of the phantom model discretized into voxels. Each voxel is considered as a focus point in the search method.

Table 3.2 gives the coordinates of the easiest/most difficult places to heat in the phantom at 500, 600, 700 and 800 MHz. The dimensions of the original tissue matrix of the spherical head phantom were $200 \times 200 \times 200$ mm^3. To avoid lengthy computation times, we decreased the resolution of the tissue matrix to 5 mm which resulted in a matrix of $40 \times 40 \times 40$ mm^3. In Table 3.2, the most difficult places to heat are those with the highest HTQ and the easiest places have the lowest HTQ values.

Table 3.2: Worst and best HTQ coordinates of 50 antennas obtained in a $40 \times 40 \times 40$ mm^3 head model. The centre of the phantom is located at the point [20,20,20].

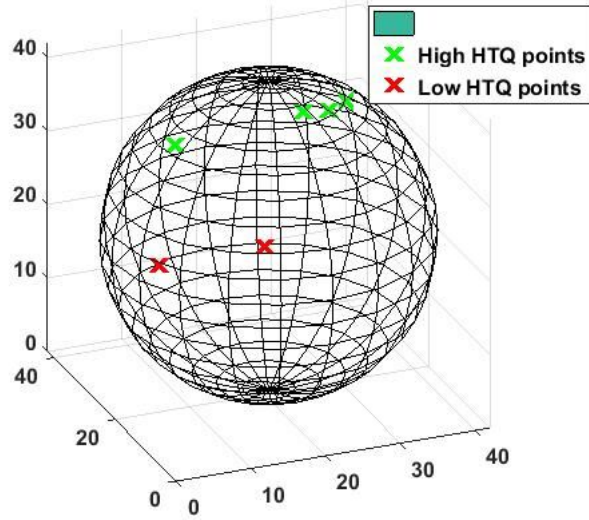| Frequency	Worst HTQ coordinates	Best HTQ coordinates
500 MHz	[8, 20, 36]	[20, 20, 20]
600 MHz	[24, 17, 39]	[6, 20, 20]
700 MHz	[31, 20, 38]	[20, 20, 20]
800 MHz	[27, 16, 39]	[20, 20, 20]

Figure 3.6: The coordinates with highest (shown in green) and lowest (shown in red) HTQ values found by using the search algorithm in the spherical phantom surrounded by 50 antennas, Figure 3.5(a).

Table 3.2 shows that the points with high HTQs are closest to the top of the phantom (the z-coordinate values close to 40 mm), while the points with lower HTQs are close to the phantom centre (z-coordinate values close to 20 mm). The position of these coordinates over a sphere of radius 20 mm is shown in Figure 3.6. The results presented in Table 3.2 show that the most difficult places to heat vary spatially with different frequencies. This shows the potential of the multi-frequency approach, which was the motivation for designing UWB antennas and applicators in this thesis.

As a next step, the complex geometry of the head is taken into account by using a realistic model of a child's head containing medulloblastoma. The sagittal plane of the head model as well as the antenna applicator are depicted in figure 3.7. The applicator design is different from the previous one in its helmet shape and the use of two different types of antenna. The antennas used are the proposed SGBT, designed to work at two operational bandwidths. The applicator consists of 23 antennas with 9, 9 and 5 antennas in the first, second and third rings respectively. The antennas in the first ring operate at a lower frequency band and therefore have greater dimensions. The operational frequencies considered for the antennas in the first ring were 350 and 400 MHz. For the conventional SGBT antennas designed for the frequency band of 450MHz-1GHz, 450, 500 and 550 MHz were considered as excitation frequencies. After calculating the E-fields of

all the antennas at selected frequencies, the search method was implemented to find the easiest/most difficult places in the head, in terms of the computed HTQ values.

(a)   (b)
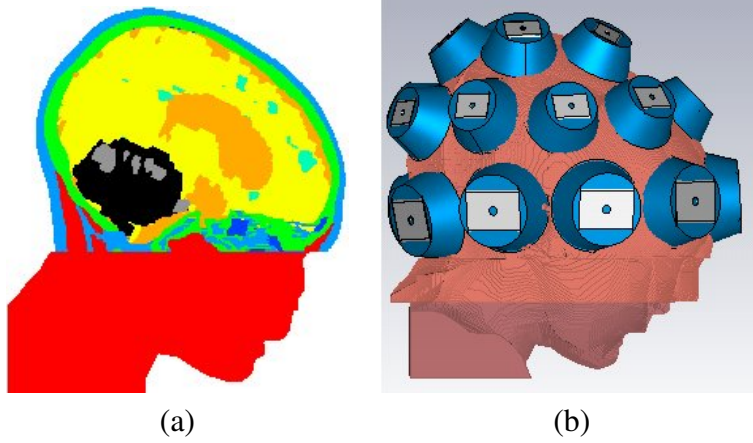
Figure 3.7: (a) Model of a child's head with a medulablastoma shown in black. (b) A helmet-shaped applicator for a child's head with 23 antennas.
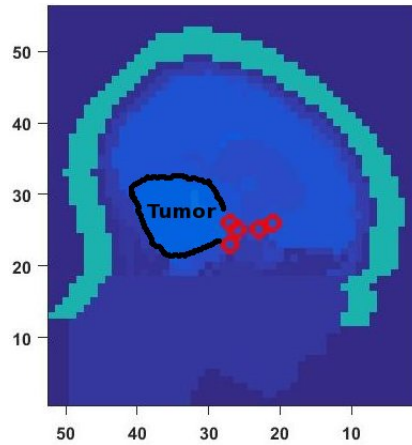
Figure 3.8: Worst HTQ places for 23 antennas obtained in a $44 \times 52 \times 56$ mm^3 head model. The figure shows locations for six different frequency combinations.

Figure 3.8 shows the most challenging locations for intraranial heating inside the child's head model at six different combinations of frequencies, representing the excitation of the scaled and regular antennas. The size of the tissue matrix including the surrounding water and air was $220 \times 260 \times 280$ mm, which was down-scaled to $44 \times 52 \times 56$ mm by a resolution of 5 mm. As shown in the

figure, the most difficult places to heat are located deep inside the head and quite close to the tumour volume. Evaluating the performance of this applicator at 350 and 500 MHz as the frequencies for the scaled and conventional antennas resulted in an HTQ value of 3.84, for the average tumour radius in the head model of about 3 cm. Likewise, the previous applicator with 50 antennas resulted in an HTQ value of about 2 to heat a similarly sized and positioned medulloblastoma in the homogeneous model. Since the calculated HTQ values indicate possible challenges to achieving suitable tumour temperatures, it is anticipated that further improvements to the current applicators will be achieved by optimising the antennas positions within them. More details regarding the optimisation of antenna positions are presented in Paper IV.

Summary of results

4.1 Paper I

This paper presents a novel concept for a self-grounded Bow-Tie-type antenna design. This is intended for use as the basic element of a phased-array applicator. The UWB operation in the frequency range of 0.43-1GHz is achieved by immersing the antenna in water bolus. The radiation characteristics are improved by appropriate shaping of the water bolus and by including dielectric layers on top of the radiating arms of the antenna.

To determine the most appropriate design, we use a combination of performance indicators representing the most important attributes of the antenna: UWB impedance matching, transmission capability and effective field size. This combination can serve as design criteria for antennas for near-field application.

Among different antenna water bolus (AWB) shapes, the optimal shape was obtained by evaluating the resulting reflection coefficient and SAR distribution of the antenna in a muscle phantom. The conical-shaped WB with optimal PLD values and S_{11} antenna parameters was selected.

The improved antenna performance (brought about by adding dielectric layers to the Bow-Tie radiating arms) is demonstrated in terms of the surface current density, E-field distribution and the reflection coefficients of the antenna, with and without dielectric layers. It is seen that, in presence of dielectric layers, higher surface current densities on the antenna arms lead to improved energy propagation into the muscle phantom. Lower absolute values of the reflection coefficient were also observed, with the added dielectric layers on the Bow-Tie radiating arms in
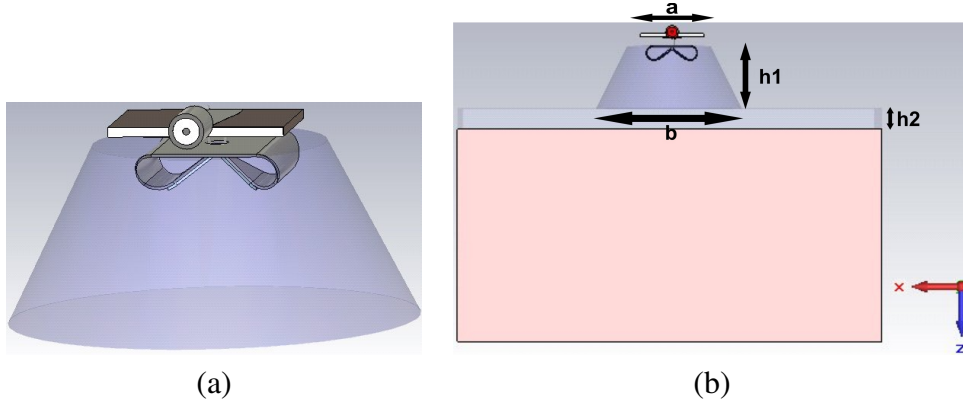
Figure 4.1: (a) Model of the self-grounded Bow-Tie antenna and (b) size parameters for the antenna water bolus.

the conical shape AWB.

In experimental validation of the antenna, the measured reflection coefficients of -9 dB or better are comparable with the simulation results in the frequency range 0.46 - 1 GHz. Finally, the heating ability of the antenna was evaluated by measuring the temperature distribution in the muscle phantom when the antenna was supplied with 10 W of power for 10 minutes. The maximum temperature increase measured by fibre optic probes was 6.5°C.

The compatibility of the antenna with an MR scanner was investigated inside a 1.5 Tesla MR scanner. Magnitude MR images of the antenna covered by WB bags show that the SMA connector with ferromagnetic material causes major image distortion. Therefore, the antenna is MR-compatible if the connector is replaced by non-magnetic one.

4.2 Paper II

This paper examined the impact of antenna numbers on the operational frequencies in an annular phased array for H&N. As a first step, the ideal frequency as a function of antenna numbers is investigated. Another question addressed is the optimum position of the virtual source in the recording stage of the time-reversal method.

Using the time-reversal method as the means of focusing, the antennas settings were determined in the range of 400-900 MHz. The antennas surrounded a homogeneous cylindrical phantom of muscle enclosing a spherical tumour. The analysis was performed for 4-48 number of antennas and tumour positions ranging from the surface to the centre of the phantom. The tumour was considered

using the same dielectric properties as the phantom and power loss density values were computed in the phantom area. The analyses were performed in the middle cut-plane of the phantom (2D), to prevent long computational times due to the high number of antennas. The optimum frequency range for each tumour position and number of antennas was determined based on the calculated aPA, the average power absorption ratio and the 50% tumour coverage. For each tumor position and number of antennas, a frequency range with a high aPA value and approximate 75% of $TC_{50\%}$ was selected.

In the second part of the paper, we carried out analyses in a 3D model of an elliptical muscle phantom enclosing a spherical tumour with the same dielectric properties as the surrounding phantom. A head applicator with 16 modified Bow-Tie antennas was considered. Based on our previous analyses, the optimum frequency range for 16 antennas was between 400-500 MHz for all tumour positions. The 50% tumour coverage was used to evaluate the heating efficiency at 400 and 500 MHz, with the tumour position varied along the Y-axis of the phantom, from surface to centre. For all the simulated frequencies, the maximum coverage for the tumour closest to the phantom centre was achieved at tumour-centre position. Finally, the optimum position of the VS was studied in realistic tumour models, with the tumour located deep inside the head. The analysis of the tongue tumour showed agreement with simple analysis results of the elliptical phantom.

4.3   Paper III

In Paper III, a laboratory prototype of an UWB hyperthermia applicator was presented and tested for treatment of tumours in the head and neck region. In the neck applicator, 10 self-grounded Bow-Tie antennas were arranged in two rings. The main reason was to decrease the smallest possible diameter of the array. Also, the diameter of the neck applicator was adjustable between 180 and 220 mm. As designed in Paper I, each antenna was placed inside a conical enclosure filled with distilled water. An extra layer of circulated distilled water was used to fill the space between the patient and the applicator to ensure matching and provide the necessary cooling of the surface. In this experiment, a thin single-inlet-single-outlet plastic bag was used as the water bolus. All antennas in the applicator operated in the frequency range of 450 MHz and 900 MHz.

The focusing capability of the applicator intended for treating neck tumours was tested on a homogeneous muscle phantom at 500 MHz. The phantom was located centrally inside the applicator. Both phantom and water bolus had initial temperatures of $20°C$, i.e. room temperature. Prior to the experiments, the phantom was cut in its centre plane in order to capture thermal images using an IR camera. The setup of the experiment is shown in Figure 4.2.
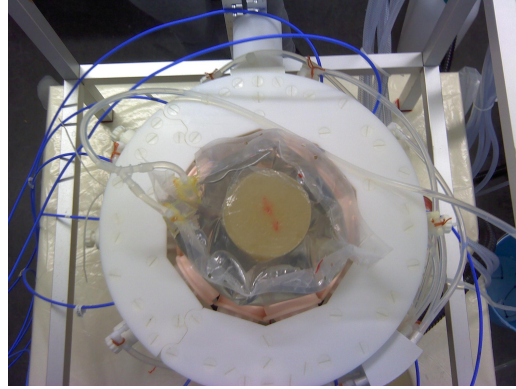
Figure 4.2: Measurement setup shows the muscle phantom surrounded by water bag and applicator.

Two tumor positions were investigated: one in the centre and one at side of the mid-transverse plane of the phantom. The time-reversal cavity was used to determine the amplitude and phase settings of the antennas. In the first experiment, the aim was to focus in the centre position. The temperature distribution in the central plain of the pre-cut muscle phantom was captured by IR camera using a 10-minute exposure. A 12°C temperature increase was obtained at the centre position. For the second experiment, the focusing was in one side of the central plane. Using the new setting at a total power output of 25 W, a maximum temperature increase of 8°C was achieved in this side position after 10 minutes radiation into the phantom. As shown in Paper III, the temperature images indicated agreement between the planned and measured focal spots, with an acceptable temperature increase in these areas.

4.4 Paper IV

In this paper, we move away from a classical, annular-phased array design to novel, helmet-shaped applicators for dedicated intracranial heating. We use the SGBT from Paper I as antenna elements in the applicators. The dimensions were scaled up by a factor of 1.6 so as to cover even lower frequencies. However, to facilitate the use of more antennas, the dimensions of the water bolus in the antennas were significantly reduced. This resulted in the operational frequencies over 314-600 MHz and 500 MHz-1 GHz respectively. First, we studied the effect of increasing the number of antennas on the average power loss density in the tumours. These were tumours located deep in the brain, at the centre and in one instance in a non-central position in a homogeneous spherical phantom with the dielectric properties of grey matter. Our simulation results revealed that increas-

ing the number of antennas, regardless of their frequency range, always resulted in higher average PLD in tumours. Moreover, heating the tumour in the centre position was easier than the non-central positions in all the applicators.

In the next part of the paper, three virtual applicators with 15, 26 and 58 Bow-Tie antennas were evaluated in terms of the calculated tumour coverage, aPA and RTMi values over the frequency range of 400-900 MHz. The results obtained indicated that applicators with more antennas produced significantly higher tumour coverage than ones with fewer antennas. This applied to both tumour positions studied. Moreover, using more antennas at higher frequencies was found to be more beneficial in increasing the power absorption in tumours than using fewer antennas at lower frequencies. For larger tumours, lower frequencies resulted in less absorbed power in healthy tissues.

4.5 Paper V

In this paper, we developed a novel method to find an optimal positioning of the antenna elements within an antenna applicator to heat a tumour of a given size and position. The applicators where the antennas were positioned was the helmet structure introduced in paper III. The initial head model was a spherical, homogeneous phantom with dielectric properties of brain grey matter surrounded by a thin water layer. To evaluate the convergence of the algorithm to the optimal solution, dipole antennas immersed in water bolus were used initially and Bow-Tie antennas were used later. The optimisation was verified with reference to the constraints on overlapping antennas. In the main part of the paper, the antenna placement was optimised to achieve the most favorable SAR distribution in a realistic model of a 13-year-old child with medulloblastoma.

46

Conclusion and outlook

This thesis has presented developments towards an optimal microwave hyperthermia applicator for treatment the head and neck as well as brain tumours. Two of the main components in a hyperthermia system have been studied: the hyperthermia applicator and hyperthermia treatment planning. Papers I and III have presented the design and experimental verification of the single antenna element and the H&N applicator. Papers II, IV and V were mainly based on the numerical modellings, simulations and optimisation, using the principle of the time-reversal method.

In the first paper, a wideband antenna was developed for use as the radiating element of the phased array hyperthermia applicator. The typically large, narrow-band antenna elements in hyperthermia applicators were replaced by a small, wide-band antenna. This meant that we could incorporate large number of antennas in the applicators which resulted in high power deposition values in the tumour, as shown and presented in Paper III. Moreover, the wideband performance provided the capability to switch over frequencies which, in turn, enabled the heating pattern of the antenna to be adapted to a specific target. The antenna was verified experimentally on a homogeneous muscle phantom. Moreover, the test of our single antenna in an MR scanner device showed its compatibility for future thermometry measurements. However, adaptation is needed to cope with the high voltage and power of an MR scanner. One method is to use high-voltage non-magnetic trimmers, placing a cable trap in the feeding cable of each antenna. This can enforce large impedance on the coaxial cable [83][84].

Paper II focused on hyperthermia treatment planning and a time-reversal method was used to find the amplitudes and phases of the antennas in the applicators. This

paper proposed a selection scheme for frequency and virtual source positioning in the time-reversal method. The results obtained, in terms of number of antennas and frequency, showed that lower operational frequencies were appropriate for applicators with fewer antennas, while higher frequencies were optimal when there were more antennas and for superficial tumours. Moreover, in the analysis to find the optimum position of the virtual source, the position of the tumour was found to be a crucial factor. A number of simplifications were made to this process. Firstly, the modeled phantom was homogeneous meaning that the presence of many tissues around the tumour was ignored. Also, the tumour was represented as a spherical homogeneous volume, which is not the case for real tumours. Also, the absence of a source with a spherical radiation pattern in CST software meant that we had to model the virtual source as a small, discreet port.

Paper III presented and tested the laboratory prototype of the hyperthermia applicator for treating head and neck tumours. Although the experiment simply proved the functionality of the time-reversal method in practice, there were a couple of issues requiring further consideration in future work. Firstly, two interchangeable hyperthermia applicators have been designed and manufactured for treatment of the head and neck tumours. To adapt the applicator diameter to the patient's neck or head size, antennas must be moved radially for each patient, which can be an unwieldy exercise. This means the water bolus between the patient and applicator needs to be redesigned for each patient, which demands a stable, reproducible water bolus design. Secondly, the water bolus in the experiment was a single-inlet-single-outlet water bag which was not an integral part of the applicator. This can result in the presence of an air gap in front of the antennas, thus causing mismatch.

The last two papers were focused on hyperthermia applicators for treating brain tumours. Paper IV presented helmet hyperthermia applicators for heating deep-seated brain tumours in children. It also investigated the effect of large numbers of antennas and low frequencies on the heating efficiency of the applicators. As with Paper II's presentation of phased array applicators, increasing the number of antennas resulted in higher average PLD in the tumour and more tumour coverage. Moreover, lower frequencies were found to be more efficient (in terms of treatment quality) at heating larger tumours than higher frequencies. To show that the simulations carried out were reasonable in the homogeneous phantom, dielectric properties of the phantom were compared and found to be similar to those of an averaged brain model. In particular, the σ was less than 8% lower than the one in the averaged homogeneous brain model. Limitations we may face in this regard arise from introducing a helmet applicator to the clinic with a large number of antenna elements (50 for example). Antenna positioning, the degree of flexibility to move or rotate over the small surface of a child's head and cross-coupling between the adjacent antenna elements are some of the possible limitations.

48

In the last paper, the optimal positioning of antennas was investigated for heating deep-seated brain tumours. The optimisation method was initially verified on a homogeneous spherical phantom and then carried out using a realistic model of a child's head. Since the optimisation was based on finding the best value of hyperthermia quality indicators, the computation of E-fields prior to the optimisation was unavoidable. However, in an applicator with a large number of antennas, this calculation is computationally expensive. Consequently, the E-fields in all the optimisation were obtained by doing a rotation of one or two pre-calculated E-fields, followed by interpolation. This resulted in approximated E-field values. Moreover, to avoid long computational times, the resolution of all the 3D matrices used was decreased. These factors may have introduced uncertainties into the final optimisation results. More limitations may arise subsequently, when manufacturing the applicator. As one of these limitations, the size of the applicator must be adapted to the head of each patient. In addition, different antenna settings are required for each patient. Moreover, in optimising the antenna positions, a certain flexibility in moving the antennas is to be expected. In designing a brain applicator with a large number of antennas, the greater level of flexibility is accompanied by greater systemic complexity. There is, nevertheless, scope to improve the heating efficiency in an applicator design. One such improvement is optimising an applicator consists of antennas with different frequency ranges. Another would be first finding the most difficult places to heat in the tumour of a patient model and then conducting the optimisation to achieve the best quality indicator for heating that place.

Bibliography

[1] Natiional cancer institute, NIH, https://www.cancer.gov/.

[2] American Cancer Society, https://www.cancer.org/.

[3] World health organization, media centre, http://www.who.int/mediacentre/factsheets/fs297/en/.

[4] National Cancer Institute: Cancer trends progress report, January 2017 - update. http://progressreport.cancer.gov.

[5] S.B. Field and C. Franconi, "Physics and Technology of Hyperthermia". Nato ASI series, Applied sciences, No 127.

[6] Coley WB. "The treatment of malignant tumors by repeated inoculation of erysipelas-with a report of ten original cases". American Journal of Medical Science. 1893; 105:489511.

[7] H. Kampinga, "Cell biological effects of hyperthermia alone or combined with radiation or drugs: a short introduction to newcomers in the field", Int. J. Hyperthermia 22 1916, 2006.

[8] J. Van der Zee, "Heating the patient: a promising approach?", *Annals of Oncology*, vol. 13, pp. 1173-1184, 2002.

[9] Z. Vujaskovic, CW. Song, "Physiological mechanisms underlying heat-induced radiosensitization", Int J Hyperthermia. 2004 Mar; 20(2): 163-74.

[10] G. Hahn, "Hyperthermia and cancer". New York: Plenum Press; 1982.

[11] WC. Dewey, "Interaction of heat with radiation and chemotherapy", Cancer Res. 1984 Oct;44(10 Suppl): pp. 4714-4720.

[12] R. Issels, E. Kampmann, R. Kanaar and L. H. Lindner, "Hallmarks of hyperthermia in driving the future of clinical hyperthermia as targeted therapy:translation into clinical application", Int J Hyperthermia. 2016 January, 32:1, pp. 89-95.

[13] SA. Sapareto and WC. Dewey, "Thermal dose determination in cancer therapy". International Journal of Radiation Oncology, Biology, and Physics 10: 787-800, 1984.

[14] Gerard C. van Rhoon, "Is CEM43 still a relevant thermal dose parameter for hyperthermia treatment monitoring?", International Journal of Hyperthermia, 2016; 32(1): 50-62.

[15] N. Cihoric, A. Tsikkinis, G. van Rhoon , H. Crezee, DM. Aebersold, S. Bodis, M. Beck, J. Nadobny, V. Budach, P. Wust, P. Ghadjar, "Hyperthermia-related clinical trials on cancer treatment within the ClinicalTrials. gov registry." *Int. J. Hyperth*, vol. 31(6), pp. 609-14. Sep 2015.

[16] N. Datta, S.Rogers, S.G. Ordonez, E. Puric and S. Bodis, "Hyperthermia and radiotherapy in the management of head and neck cancers: A systematic review and meta-analysis", Int. J. Hyperthermia 32 31-40, 2016.

[17] P. Wust, B. Hildebrandt, G. Sreenivasa, B. Rau, J. Gellermann, H. Riess, R. Felix and PM. Schlag. "Hyperthermia in combined treatment of cancer". THE LANCET Oncology Vol. 3 August 2002.

[18] N.R. Datta, S. G. Ordonez, U.S. Gaipl, M.M. Paulides, H. Crezee, J. Gellermann, D. Marder,E. Puric, S. Bodis. "Local hyperthermia combined with radiotherapy and-/or chemotherapy: Recent advances and promises for the future". Cancer Treat Rev. 2015 Nov;41(9):742-53. doi: 10.1016/j.ctrv.2015.05.009. Epub 2015 May 27.

[19] Matthew Mallory, Emile Gogineni, Guy C. Jones, Lester Greer, Charles B. Simone II. "Therapeutic hyperthermia: The old, the new, and the upcoming". Crit Rev Oncol Hematol. 2016 Jan;97:56-64. doi: 10.1016/j.critrevonc.2015.08.003. Epub 2015 Aug 8.

[20] M. M. Paulides, G. M. Verduijn, N. Van Holthe, "Status quo and directions in deep head and neck hyperthermia". Radiation Oncology 2016 11: 21.

[21] M. Van Holte, M. Paulides, D. de Jong, A. Aangeenbrug, G. van RHoon, M. Franckena, G. Verdujn. Dept. Radiation Oncology, Erasmus MC Cancer

Institute Rotterdam, The Netherlands, "Early experience with HYPERcollar3D applicator as radiosentisizer for tumors in head and neck region", Esho Annual Meeting, June 2015, Switzerland.

[22] R. Issels, "Hyperthermia adds to chemotherapy", *Eur. J. Cancer*, vol. 44, pp. 2546-54, 2008.

[23] O. Dahl, R. Dalene, B. C. Schem, O. Mella, "Status of clinical hyperthermia", *Acta Oncol.*, vol. 38, no. 7, pp. 863-873, 1999.

[24] M. Amichetti, M. Romano, L. Busana, A. Bolner, G. Fellin, G. Pani, L. Tomio and R. Valdagni, "Hyperfractionated radiation in combination with local hyperthermia in the treatment of advanced squamous cell carcinoma of the head and neck: a phase I-II study" Radiother Oncol. 45 155-8, Nov 1997.

[25] M. Franckena, D. Fatehi, M. Bruijne, R. Canters, Y. Norden, J. Mens, G. Rhoon and J. Zee, "Hyperthermia dose-effect relationship in 420 patients with cervical cancer treated with combined radiotherapy and hyperthermia" Eur. J. Cancer 45 1969-78 2009.

[26] Van der Zee, D. Gonzales Gonzales, G.C. Van Rhoon et al., "Comparison of radiotherapy alone with radiotherapy plus hyperthermia in locally advanced pelvic tumours: a prospective, randomised, multicentre trial", Lancent, Volume 355, Issue 9210, 1 April 2000, Pages 1119-1125.

[27] RD. Issels, LH. Lindner, J. Verweij, P. Wust, P. Reichardt, BC. Schem, S. Abdel-Rahman, S. Daugaard, C. Salat, CM. Wendtner, Z. Vujaskovic, R. Wessalowski, KW. Jauch, HR. Drr, F. Ploner , A. Baur-Melnyk , U. Mansmann , W. Hiddemann, JY. Blay, P. Hohenberger, "Neo-adjuvant chemotherapy alone or with regional hyperthermia for localised high-risk soft-tissue sarcoma: a randomised phase 3 multicentre study". Lancet Oncol. 2010 Jun; 11(6): 561-70. doi: 10.1016/S1470-2045(10)70071-1. Epub 2010 Apr 29.

[28] Globocan 2012: Estimated cancer incidence, mortality and prevalence worlwide in 2012. URL http://globocan.iarc.fr/Pages/fact_sheets_population.aspx, accessed 09-10-2017.

[29] B. A. Conley, "Treatment of Advanced Head and Neck Cancer: What Lessons Have We Learned?". Journal of clinical oncology, volume 24, number 7, March 2006.

[30] Pignon JP., Bourhis J., Domenge C., Designe L. "Chemotherapy added to locoregional treatment for head and neck squamous-cell carcinoma: three meta-analyses of updated individual data". MACH-NC Collaborative Group. Meta-Analysis of Chemotherapy on Head and Neck Cancer. Lancet. 2000; 355(9208): 949-55.

[31] Pignon JP, le Maitre A, Maillard E, Bourhis J, Group M-NC. "Meta-analysis of chemotherapy in head and neck cancer (MACH-NC): an update on 93 randomised trials and 17,346 patients". Radiother Oncol. 2009; 92(1): 4-14.

[32] R. Valdagni, M. Amichetti, G. Pani, "Radical radiation alone versus radical radiation plus microwave hyperthermia for N3 (TNM-UICC) neck nodes: a prospective randomized clinical trial" *Int. J. Radiat. Oncol. Biol. Phys.*, vol. 15, pp. 13-24, 1988.

[33] R. Valdagni, M. Amichetti, "Report of long-term follow-up in a randomized trial comparing radiation therapy and radiation therapy plus hyperthermia to metastatic lymphnodes in stage IV head and neck patients" *Int. J. Radiat Oncol Biol Phys*, 1993; vol. 28, pp. 163-169, 1993.

[34] H. Yan, DW. Parsons, G. Jin, et al. "IDH1 and IDH2 mutations in gliomas". N Engl J Med. 2009; 360(8): 765-773.

[35] BC. Christensen, AA. Smith, S. Zheng, et al. "DNA methylation, isocitrate dehydrogenase mutation, and survival in glioma". J Natl Cancer Inst. 2011; 103(2): 143-153.

[36] I. Qaddoumi, I. Sultan, A. Gajjar, Outcome and prognostic features in pediatric gliomas: a review of 6212 cases from the Surveillance, Epidemiology, and End Results database. Cancer. 2009; 115(24): 5761-5770.

[37] David W. Ellison, "Childhood medulloblastoma: novel approaches to the classification of a heterogeneous disease", Acta Neuropathol (2010) 120: 305-316.

[38] G. Gustafsson, M. Heyman and A Vernby, "Childhood Cancer Incidence and Survival in Sweden 19842005", Karolinska Institutet, Stockholm, pp. 2007.

[39] B. Lannering, I. Marky, A. Lundberg et al. "Long-term sequelae after pediatric brain tumors", *Medical and pediatric oncology*, vol. 18, pp. 304-310, 1990.

[40] M. Salcman, GM. Samaras, "Interstitial microwave hyperthermia for brain tumors." *J Neuro-Oncology*, 1(3), pp. 225-236, 1983.

[41] A. Winter, M.D.J. Laing, R. Paglione, F. Sterzer, "Microwave Hyperthermia for Brain Tumors", Neurosurgery, Vol. 17(3), pp. 387-399, 1985.

[42] PK. Sneed, PR. Stauffer, MW. McDermott, CJ. Diederich, KR. Lamborn, MD. Prados, S. Chang, KA. Weaver, L. Spry, MK. Malec, SA. Lamb, B. Voss, RL. Davis, WM. Wara, DA. Larson, TL. Phillips, PH. Gutin. "Survival benefit of hyperthermia in a prospective randomized trial of brachytherapy boost +/- hyperthermia for glioblastoma multiforme", Int J Radiat Oncol Biol Phys. 1998 Jan 15; 40(2): 287-95.

[43] S. Jiahang, G. Mian, P. Hengyuan, Q. Jingtao, Z. Jinwei, and G. Yunlong, "Treatment of malignant glioma using hyperthermia", Neural Regen Res. 2013 Oct 15; 8(29): 2775-2782.

[44] H.P. Kok, "Treatment planning for locoregional and intraluminal hyperthermia", PhD thesis, Universiteit van Amsterdam, April 2007.

[45] K. Maier-Hauff, F. Ulrich, D. Nestler, et al. "Efficacy and safety of intratumoral thermotherapy using magnetic iron-oxide nanoparticles combined with external beam radiotherapy on patients with recurrent glioblastoma multiforme." *J Neurooncol*, vol. 103(2), pp. 317-24, 2011.

[46] M. Wankhede, A. Bouras, M. Kaluzova, and C. G Hadjipanayis, "Magnetic nanoparticles: an emerging technology for malignant brain tumor imaging and therapy", Expert Rev Clin Pharmacol. 2012 Mar; 5(2): 173-186.

[47] R. Hergt, S. Dutz, M. Zeisberger. "Validity limits of the Neel relaxation model of magnetic nanoparticles for hyperthermia", Nanotechnology. 2010; 21:015706. PubMed: 19946160.

[48] K. Hynynen, RM. Jones, "Image-guided ultrasound phased arrays are a disruptive technology for non-invasive therapy.", *Phys Med Biol*, 61(17): R206-48, 2016.

[49] Z. Ram, ZR. Cohen, S. Harnof, S. Tal, M. Faibel, D. Nass, SE. Maier, M. Hadani, Y. Mardor, "Magnetic resonance imaging-guided, high-intensity focused ultrasound for brain tumor therapy", *Neurosurgery*, 59(5): 949-55, 2006.

[50] J. Jagannathan, N. K Sanghvi, L. A Crum, C. Yen, R. Medel, A. S Dumont, J. P Sheehan, L. Steiner, F. Jolesz and N. F Kassell, "High intensity

focused ultrasound surgery (HIFU) of the brain: A historical perspective, with modern applications", NIH Public Access, Author Manuscript.

[51] ZR. Cohen, J. Zaubermann, S. Harnof, Y. Mardor, D. Nass, E. Zadicario, A. Hananel, D. Castel, M. Faibel, Z. Ram. "Magnetic resonance imaging-guided focused ultrasound for thermal ablation in the brain: a feasibility study in a swine model". Neurosurgery. 2007; 60:593-600. discussion 600. [PubMed: 17415195].

[52] Wessalowski R. "The Role of Hyperthermia in Pediatric Oncology Cap. 4 in Hyperthermia in Oncology- Principles and Therapeutic Outlook/ Oliver J. Ott, Rolf D. Issels, Rdiger Wessalowski.- 1st edition-Bremen: Uni-Med 2010.

[53] R. Wessalowski, DT. Schneider, O. Mils, V. Friemann, O. Kyrillopoulou, J. Schaper, C. Matuschek, K. Rothe, I. Leuschner, R. Willers, S. Schnberger, U. Gbel, G. Calaminus; MAKEI study group, "Regional deep hyperthermia for salvage treatment of children and adolescents with refractory or recurrent non-testicular malignant germ-cell tumours: an open-label, non-randomised, single-institution, phase 2 study", Lancet Oncol. 2013 Aug; 14(9): 843-52.

[54] R. Wessalowski, R. Canters, G. C. van Rhoon, "EMF hyperthermia in Children", Conference: Microwave Conference (EuMC), 2012 42nd European.

[55] B. Gurin, J. F. Villena, A. G. Polimeridis, E. Adalsteinsson, L. Daniel, J. K. White, B. R. Rosen and L. L.Wald, "Computation of ultimate SAR amplification factors for radiofrequency hyperthermia in non-uniform body model: impact of frequency and tumour location". accepted in Int. J. Hyperthermia 2017, available online in http://dx.doi.org/10.1080/02656736.2017.1319077.

[56] K. D. Paulsen, S. Geimer, J. Tang and W. E. Boyse, "Optimization of pelvic heating rate distributions with electromagnetic phased arrays" Int. J. Hyperth. 15 157-86, 1999.

[57] P. Wust, M. Seebass, J. Nadobny, P. Deuflhard, G. Monich and R. Felix, "Simulation studies promote technological development of radiofrequency phased array hyperthermia", Int. J. Hyperth. 1996; 12 477-94.

[58] M. M. Paulides, J. F. Bakker, A. P. M. Zwamborn, & G. C. VAN Rhoon, "A head and neck hyperthermia applicator: Theoretical antenna array design", Int. J. Hyperthermia, February 2007; 23(1): 59-67.

[59] J. D. P. Van Dijk, D. Gonzalez-Gonzalez and L. E. C. M. Blank, "Deep local hyperthermia with a four aperture array system of large waveguide radiators. results of simulation and clinical application" Hyperthermic Oncology 1988 ed T Sugahara and M Saito (London: Taylor and Francis) pp. 573-5.

[60] P. F. Turner and T. Schaeffermeyer, "BSD-2000 approach for deep local and regional hyperthermia" Strahlenther. Onkol. 165 738-4, 1989.

[61] H.D. Trefna, H. Crezee, M. Schmidt, D. Marder et al. "Quality assurance guidelines for superficial hyperthermia clinical trials: I. Clinical requirements", Int J Hyperthermia. 2017 Jan 31: 1-12.

[62] G. Bruggmoser, S. Bauchowitz, R. Canters et al. "Guideline for the clinical application, documentation and analysis of clinical studies for regional deep hyperthermia", Strahlenther Onkol (2012) 188(Suppl 2): 198. https://doi.org/10.1007/s00066-012-0176-2.

[63] M. Gautherie, "Methods of External Hyperthermic Heating". Clinical Thermology, Springer-Verlag 1990.

[64] HP. Kok, P. Wust, PR. Stauffer, F. Bardati, GC. van Rhoon, J. Crezee. "Current state of the art of regional hyperthermia treatment planning: a review". RadiatOncol. 2015; 10(1): 196.

[65] G.C. Van Rhoon, P. Wust, "Introduction: non-invasive thermometry for thermotherapy", Int J Hyperthermia. 2005 Sep; 21(6): 489-95.

[66] L. Winter, E. Oberacker, K. Paul, Y. Ji, C. Oezerdem, P. Ghadjar, A. Thieme, V. Budach, P. Wust, T. Niendorf, "Magnetic resonance thermometry: Methodology, pitfalls and practical solutions", Int J Hyperthermia. 2016;32(1): 63-75.

[67] David K. Cheng, "Field and Wave Electromagnetics", second Edition, 1989 by Addison-Wesley Publishing Company, Inc.

[68] Lee CK. Song CW. Rhee JG. Foy JA. and Levitt SH. "Clinical experience using 8 MHz radiofrequency capacitive hyperthermia in combination with radiotherapy: Results of a phase I/II study". International Journal of Radiation Oncology, Biology, and Physics 32: 733-745, 1995.

[69] R. Magin and A. Peterson, "Noninvasive microwave phased arrays for local hyperthermia: a review". Int J Hyperthermia, 5: 429-450, 1989.

[70] F. Jouvie, JC. Bolomey, and G. Gaboriaud, "Discussion of the capabilities of microwave phased arrays for hyperthermia treatment of neck tumors". IEEE Trans Micr Theor Tech, 34: 495-501, 1986.

[71] M. M. Paulides, J.F. Bakker, E. Neufeld, J. van der Zee, P.P Jansen, P.C. Levendag, G. C. van Rhoon, "The HYPERcollar: A novel applicator for hyperthermia in the head and neck", *Int J Hyperthermia*, vol. 23, pp. 567-76, 2007.

[72] M. M. Paulides, J.F. Bakker, E. Neufeld, J. van der Zee, P.P Jansen, P.C. Levendag, G. C. van Rhoon, "Clinical Introduction of Novel Microwave Hyperthermia Technology: the HYPERcollar3D Applicator for Head and Neck Hyperthermia", *9th European Conference on Antennas and propagation*, EuCAP 2015, Lisbon, Portugal.

[73] H.P. Kok, M. de Greef, J. Wiersma, A. Bel and J. Crezee, "The impact of the waveguide aperture size of the 3D 70 MHz AMC-8 locoregional hyperthermia system on tumor coverage", Phys. Med. Biol.55(2010) 4899-4916.

[74] ALBA hyperthermia system, http://www.albahyperthermia.com.

[75] Pyrexar medical, http://www.pyrexar.com.

[76] R.A.M.Canters, M.M.Paulides, M.Franckena, J.W.Mens, G.C.vanRhoon, "Benefit of replacing the Sigma-60 by the Sigma-Eye applicator. A Monte Carlo-based uncertainty analysis", Strahlentherapie und Onkologie January 2013, Volume 189, Issue 1, pp. 74-80.

[77] Craciunescu O. Blackwell K. Jones E. et al. (2009a) DCE-MRI parameters have potential to predict response of locally advanced breast cancer patients to neoadjuvant chemotherapy and hyperthermia: A pilot study. International Journal of Hyperthermia 25: 405-415.

[78] P. Wust, H. Fähling, W. Wlodarczyk, M. Seebass, J. Gellermann, P. Deuflhard, J. Nadobny, "Antenna arrays in the SIGMA-eye applicator: interactions and transforming networks", *Med. Phys.*, vol. 28, pp. 1793-805, 2001.

[79] M. M. Paulides, J. F. Bakker, N. Chavannes, G. C. Van Rhoon, "A patch antenna design for application in a phased-array head and neck hyperthermia applicator", *IEEE Transactions On Biomedical Engineering*, vol. 54, no. 11, November 2007.

58

[80] H. D. Trefná, J. Vrba, M. Persson, "Evaluation of a patch antenna applicator for time reversal hyperthermia", Int. J. Hyperthermia, pp. 185-197, March 2010.

[81] H. Dobšíček Trefná, A. Imtiaz, H. S. Lui, T. Rubaek, M. Persson, "Evolution of an UWB antenna for hyperthermia array applicator", *6th European Conference on Antennas and Propagation*, pp. 1046-1048, March 2012.

[82] L. Winter, C. Ozerdem, W. Hoffmann, D. Santoro, A. Muller, H. Waiczies, R. Seemann, A. Graessl, P. Wust, T. Niendorf. "Design and Evaluation of a Hybrid Radiofrequency Applicator for Magnetic Resonance Imaging and RF Induced Hyperthermia: Electromagnetic Field Simulations up to 14.0 Tesla and Proof-of-Concept at 7.0 Tesla", in PLOS ONE, Volume 8, Issue 4, April 2013.

[83] M.M. Paulides, W.CM Numan, T. Drizdal, G. Kotek, DTB Yeo, GC. Van Rhoon. "Feasibility of MRI-guided Hyperthermia Treatment of Head and Neck Cancer", European Conference on Antennas and Propagation, April 2014.

[84] JJW. Lagendijk, "A new coaxial TEM radio-frequency/microwave applicator for non-invasive deep-body hyperthermia", J Microwave Power 18:367-375, 1983.

[85] M.M. Paulides,R.R. Stauffer, e. Neufeld, P.F. Maccarini, A. Kyriakou, R.A.M. Canters, C.J. Diederich, J.F. Bakker and G.C. Van Rhoon," Simulation techniques in hyperthermia treatment planning, Int J Hyperthermia, vol. 29(4), pp. 346-357. 2013.

[86] CST- Computer Simulation Technology. Retrieved from https://www.cst.com/Products/CSTMWS.

[87] Fortunati V. Verhaart RF. Van der Lijn F. Niessen WJ, Veenland JF. Paulides MM. et al. "Tissue segmentation of head and neck CT images for treatment planning: A multi-atlas approach combined with intensity modeling". Med Phys, in press.

[88] R. F. Verhaart, V. Fortunati, G. M. Verduijn, A. van der Lugt, T. van Walsum, J. F. Veenland, and M. M. Paulides "The relevance of MRI for patient modeling in head and neck hyperthermia treatment planning: A comparison of CT and CT-MRI based tissue segmentation on simulated temperature", Med Phys. 2014 Dec; 41(12).

[89] K. R. Foster and H. P. Schwan, "Dielectric properties of tissues and biological materials: A critical review" Crit. Rev. Biomed. Eng.17 25-104, 1989.

[90] C. Gabriel, S. Gabriel and E. Corthout, "The dielectric properties of biological tissues: I. Literature survey", 1996 Phys. Med. Biol. 41 2231.

[91] S. Gabriel, R. W. Lau and C. Gabriel, "The dielectric properties of biological tissues: II. Measurement in the frequency range 10 Hz to 20 GHz" Phys. Med. Biol.41 2251-69, 1996b.

[92] S. Gabriel, R. W. Lau and C. Gabriel, "The dielectric properties of biological tissues: III. Parametric models for the dielectric spectrum of tissues" Phys. Med. Biol.41 (1996) 2271-2293.

[93] W. D. Hurt, "Multiterm Debye dispersion relations for permittivity of muscle" IEEE Trans. Biomed. Eng.32 60-4, 1985.

[94] P. Debye, Ver. Deut. Phys. Gesell. 15, 777; reprinted 1954 in collected papers of Peter J.W. Debye Interscience, New York, 1913.

[95] K.S. Cole; R.H. Cole. "Dispersion and Absorption in Dielectrics - I Alternating Current Characteristics". J. Chem. Phys. 9: 341-352, 1941.

[96] M. De Greef, HP. Kok, D. Correia, PP. Borsboom, A. Bel, J. Crezee, "Uncertainty in hyperthermia treatment planning: The need for robust system design". Phys Med Biol 2011; 56: 3233-50.

[97] F. Bardati, A. Borrani, A. Gerardino and G. A. Lovisolo, "SAR Optimization in a Phased Array Radiofrequency Hyperthermia System", IEEE transactions on biomedical engineering, Vol. 42, No. 12, December 1995.

[98] T. Köhler, P. Maass, P. Wust, M. Seebass, "A fast algorithm to find optimal controls of multiantenna applicators in regional hyperthermia", Phys Med Biol. 2001 Sep; 46(9): 2503-14.

[99] N. Siauve, L. Nicolas, C. Vollaire, A. Nicolas, and J.A. Vasconcelos, "Optimization of 3-D SAR Distribution in Local RF Hyperthermia", IEEE Transactions on Magnetics, Vol. 40, No. 2, March 2004.

[100] Z. Rijnen, GC. van Rhoon, JF Bakker, RAM. Canters, P. Togni, MM. Paulides. "Introducing VEDO for complaint adaptive hyperthermia in the head and neck". Int J Hyperthermia 2013; 29: 181-93.

[101] D. Sullivan, "Mathematical Methods for Treatment Planning in Deep Regional Hyperthermia", IEEE transactions on microwave theory and techniques, Vol. 39, No. 5, May 1991.

[102] H. H. Pennes. "Analysis of tissue and arterial blood temperatures in the resting human forearm". J App Phys 1948; 1: 93-122.

[103] J. Lang, B. Erdmann, M. Seebass, "Impact of nonlinear heat transfer on temperature control in regional hyperthermia". IEEE Trans Biomed Eng 1999; 46: 1129-38.

[104] J. Crezee, J. Mooibroek, JJ. Lagendijk, GM van Leeuwen, "The theoretical and experimental evaluation of the heat balance in perfused tissue". Phys Med Biol 1994; 39: 813-32.

[105] AN. Kotte, GM. van Leeuwen, JJ. Lagendijk, "Modeling the thermal impact of a discrete vessel tree". Phys Med Biol 1999; 44: 57-74.

[106] H.P. Kok, C.A.T. van den Berg, A. Bel and J. Crezee, "Fast thermal simulations and temperature optimization for hyperthermia treatment planning, including realistic 3D vessel networks", Med Phys. 2013 Oct.

[107] M. de Greef, H. P. Kok, D. Correia, A. Bel, and J. Crezee, "Optimization in hyperthermia treatment planning: the impact of tissue perfusion uncertainty", Med Phys. 2010 Sep; 37(9): 4540-50.

[108] RA. Canters, P. Wust, JF. Bakker, GC. Van Rhoon, "A literature survey on indicators for characterization and optimization of SAR distributions in deep hyperthermia, a plea for standardization", International Journal of Hyperthermia Volume 25, Issue 7, 2009.

[109] R. A. M. Canters, M. Franckena, M. M. Paulides, G. C. Van Rhoon, "Patient positioning in deep hyperthermia: Influences of inaccuracies, signal correction possibilities and optimization potential". Phys Med Biol. 2009; 54: 3923-36.

[110] Z. Rijnen, J.F. Bakker, R.A.M. Canters, P. Togni, G.M. Verduijn, P.C. Levendag, G.C. Van Rhoon, and M.M. Paulides, "Clinical integration of software tool VEDO for adaptive and quantitative application of phased array hyperthermia in the head and neck", Int J Hyperthermia, vol. 29(3). pp. 181-193, May 2013.

[111] M. W. Dewhirst, B. L. Viglianti, M. Lora-Michiels, M. Hanson and P. J. Hoopes, "Basic principles of thermal dosimetry and thermal thresholds for

tissue damage from hyperthermia", International Journal of Hyperthermia, Jul 2009, 19:3, 267-294.

[112] WC. Dewey, "Arrhenius relationships from the molecule and cell to the clinic". International Journal of Hyperthermia 25: 3-20, 2009.

[113] M. Fink, "Time Reversal of Ultrasonic Fields-Part I: Basic Principles", IEEE Transactions on Ultrasonic, Ferroelectrics and Frequency control, Vol. 39, No. 5, September 1992.

[114] H. D. Trefná, J. Vrba, M. Persson, "Time-reversal focusing in microwave hyperthermia for deep seated tumors", Phys. Med. Biol, pp. 2167-2185, April 2010.

[115] J. de Rosny, G. Lerosey, A. Tourin, M. Fink, "Modeling and Computations in Electromagnetics". Lecture Notes in Computational Science and Engineering, Volume 59, 2008, pp. 187-202.

[116] J. Gellermann, W. Wlodarczyk, A. Feussner, H. Fhling, J. Nadobny, B. Hildebrandt, R. Felix, and P. Wust, " Methods and potentials of magnetic resonance imaging for monitoring radiofrequency hyperthermia in a hybrid system", Int J Hyperthermia, vol. 21, No. 6, pp. 497-513, 2005.

[117] H. Dobšíček Trefná, J. Jonsson, B. Vessman, J. Wanemark, E. Woxlin, A. Hjalmarson, L. Adelback, J. Gellermanny, P. Takook, B. Lannering, K. Blomgren and M. Persson, "Antenna applicator for microwave hyperthermia treatment of pediatric brain cancer", *EuCAP 2014*, The Hague, The Netherlands, April 2014.

[118] PA. Hasgall, F. Di Gennaro, C. Baumgartner, E. Neufeld, MC. Gosselin, D. Payne, A. Klingenböck, N. Kuster, "IT'IS Database for thermal and electromagnetic parameters of biological tissues" Version 3.0, September 01st, 2015, DOI: 10.13099/VIP21000-03-0.

[119] F. Bardati, P. Tognolatti, "Hyperthermia phased arrays pre-treatment evaluation", International Journal of Hyperthermia, 32:8, 911-922, 2016.